cells (Orlicky and Schaack, 2001), although the vector in the present study contained fiber that was genetically modified with polylysine (a stretch of seven lysine residues), while their vector is just a complex of Ad and polylysine. 3T3-L1 cells might produce a large number of negatively charged glycosaminoglycans.

PPARγ is a master regulator of adipogenesis and plays an important role in the regulation of insulin sensitivity and glucose homeostasis (Tontonoz et al., 1994b; Wu et al., 1998; Kubota et al., 1999; Berger and Moller, 2002). The inhibition of preadipocyte-to-adipocyte differentiation by the silencing of PPARγ expression in 3T3-L1 cells suggests that the fiber-modified Ad vector-mediated RNAi could be widely used for the basic study of adiposity and diabetes.

Homozygous PPARγ-null mice are embryonically lethal due to placental dysfunction. Heterozygous mice (PPARγ$^{+/-}$) and conditional knockout mice have been used to study the function of PPARγ under in vivo conditions (Kubota et al., 1999). However, generation of these mice is time-consuming. In the heterozygous mice (PPARγ$^{+/-}$), the expression levels of PPARγ$^{+/-}$ cannot be regulated and are half those of the wild-type mice. Since the Ad vectors mediate efficient gene transduction even under in vivo conditions, conditional PPARγ knockdown mice might be generated by the direct in vivo injection of Ad vectors containing the siRNA expression cassette for PPARγ. Knockdown levels of PPARγ expression could be regulated by adjusting the dose of the vector. Koo et al. recently produced PGC-1 (PPARγ coactivator-1) knockdown mice by Ad delivery of PGC-1 RNAi to the liver (Koo et al., 2004).

In conclusion, the fiber-modified Ad vectors containing polylysine peptides mediate efficient gene transfer into 3T3-L1 preadipocytes and adipocytes. RNAi of PPARγ by the delivery of modified Ad vectors suppresses the preadipocyte-to-adipocyte differentiation in 3T3-L1 cells. Ad vector-mediated RNAi for PPARγ should be useful for not only studying the biological and physiological mechanism of PPARγ during adipogenesis in adiposity and diabetes, but also in therapeutic application to these and other diseases.

Acknowledgements

References

Berger, J., Moller, D.E., 2002. The mechanisms of action of PPARs. Annu. Rev. Med. 53, 409–435.

Brummelkamp, T.R., Bernards, R., Agami, R., 2002. A system for stable expression of short interfering RNAs in mammalian cells. Science 296, 550–553.

Carlotti, F., et al., 2004. Lentiviral vectors efficiently transduce quiescent mature 3T3-L1 adipocytes. Mol. Ther. 9, 209–217.

Cohen, C.J., Shieh, J.T., Pickles, R.J., Okegawa, T., Hsieh, J.T., Bergelson, J.M., 2001. The coxsackievirus and adenovirus receptor is a transmembrane component of the tight junction. Proc. Natl. Acad. Sci. U. S. A. 98, 15191–15196.

Dmitriev, I., et al., 1998. An adenovirus vector with genetically modified fibers demonstrates expanded tropism via utilization of a coxsackievirus and adenovirus receptor-independent cell entry mechanism. J. Virol. 72, 9706–9713.

Elbashir, S.M., Harborth, J., Lendeckel, W., Yalcin, A., Weber, K., Tuschl, T., 2001. Duplexes of 21-nucleotide RNAs mediate RNA interference in cultured mammalian cells. Nature 411, 494–498.

Gaggar, A., Shayakhmetov, D.M., Lieber, A., 2003. CD46 is a cellular receptor for group B adenoviruses. Nat. Med. 9, 1408–1412.

Gregoire, F.M., Smas, C.M., Sul, H.S., 1998. Understanding adipocyte differentiation. Physiol. Rev. 78, 783–809.

Havenga, M.J., et al., 2001. Improved adenovirus vectors for infection of cardiovascular tissues. J. Virol. 75, 3335–3342.

Honda, T., et al., 2000. The coxsackievirus-adenovirus receptor protein as a cell adhesion molecule in the developing mouse brain. Brain Res. Mol. Brain Res. 77, 19–28.

Hosono, T., et al., 2004. Adenovirus vector-mediated doxycycline-inducible RNA interference. Hum. Gene Ther. 15, 813–819.

Katayama, K., et al., 2004. RNA interfering approach for clarifying the PPARgamma pathway using lentiviral vector expressing short hairpin RNA. FEBS Lett. 560, 178–182.

Koizumi, N., Mizuguchi, H., Utoguchi, N., Watanabe, Y., Hayakawa, T., 2003. Generation of fiber-modified adenovirus vectors containing heterologous peptides in both the HI loop and C terminus of the fiber knob. J. Gene Med. 5, 267–276.

Koo, S.H., et al., 2004. PGC-1 promotes insulin resistance in liver through PPAR-alpha-dependent induction of TRB-3. Nat. Med. 10, 530–534.

Krasnykh, V.N., Mikheeva, G.V., Douglas, J.T., Curiel, D.T., 1996. Generation of recombinant adenovirus vectors with modified fibers for altering viral tropism. J. Virol. 70, 6839–6846.

Kubota, N., et al., 1999. PPAR gamma mediates high-fat diet-induced adipocyte hypertrophy and insulin resistance. Mol. Cell 4, 597–609.

Maizel Jr., J.V., White, D.O., Scharff, M.D., 1968. The polypeptides of adenovirus: I. Evidence for multiple protein components in the virion and a comparison of types 2, 7A, and 12. Virology 36, 115–125.

McManus, M.T., Sharp, P.A., 2002. Gene silencing in mammals by small interfering RNAs. Nat. Rev. Genet. 3, 737–747.

Miyagishi, M., Taira, K., 2002. U6 promoter-driven siRNAs with four uridine 3′ overhangs efficiently suppress targeted gene expression in mammalian cells. Nat. Biotechnol. 20, 497–500.

Mizuguchi, H., Hayakawa, T., 2002. Adenovirus vectors containing chimeric type 5 and type 35 fiber proteins exhibit altered and expanded tropism and increase the size limit of foreign genes. Gene 285, 69–77.

Mizuguchi, H., Kay, M.A., 1998. Efficient construction of a recombinant adenovirus vector by an improved in vitro ligation method. Hum. Gene Ther. 9, 2577–2583.

Mizuguchi, H., Kay, M.A., 1999. A simple method for constructing E1- and E1/E4-deleted recombinant adenoviral vectors. Hum. Gene Ther. 10, 2013–2017.

Mizuguchi, H., et al., 2001. A simplified system for constructing recombinant adenoviral vectors containing heterologous peptides in the HI loop of their fiber knob. Gene Ther. 8, 730–735.

Niwa, H., Yamamura, K., Miyazaki, J., 1991. Efficient selection for high-expression transfectants with a novel eukaryotic vector. Gene 108, 193–199.

Ntambi, J.M., Young-Cheul, K., 2000. Adipocyte differentiation and gene expression. J. Nutr. 130, 3122S–3126S.

Orlicky, D.J., Schaack, J., 2001. Adenovirus transduction of 3T3-L1 cells. J. Lipid Res. 42, 460–466.

Orlicky, D.J., DeGregori, J., Schaack, J., 2001. Construction of stable coxsackievirus and adenovirus receptor-expressing 3T3-L1 cells. J. Lipid Res. 42, 910–915.

Paul, C.P., Good, P.D., Winer, I., Engelke, D.R., 2002. Effective expression of small interfering RNA in human cells. Nat. Biotechnol. 20, 505–508.

Ross, S.A., Song, X., Burney, M.W., Kasai, Y., Orlicky, D.J., 2003. Efficient adenovirus transduction of 3T3-L1 adipocytes stably expressing coxsackie-adenovirus receptor. Biochem. Biophys. Res. Commun. 302, 354–358.

Segerman, A., Atkinson, J.P., Marttila, M., Dennerquist, V., Wadell, G., Arnberg, N., 2003. Adenovirus type 11 uses CD46 as a cellular receptor. J. Virol. 77, 9183–9191.

Shayakhmetov, D.M., Papayannopoulou, T., Stamatoyannopoulos, G., Lieber, A., 2000. Efficient gene transfer into human CD34(+) cells by a retargeted adenovirus vector. J. Virol. 74, 2567–2583.

Shen, C., Buck, A.K., Liu, X., Winkler, M., Reske, S.N., 2003. Gene silencing by adenovirus-delivered siRNA. FEBS Lett. 539, 111–114.

Short, J.J., Pereboev, A.V., Kawakami, Y., Vasu, C., Holterman, M.J., Curiel, D.T., 2004. Adenovirus serotype 3 utilizes CD80 (B7.1) and CD86 (B7.2) as cellular attachment receptors. Virology 322, 349–359.

Sui, G., Soohoo, C., Affarel, B., Gay, F., Shi, Y., Forrester, W.C., 2002. A DNA vector-based RNAi technology to suppress gene expression in mammalian cells. Proc. Natl. Acad. Sci. U. S. A. 99, 5515–5520.

Tontonoz, P., Hu, E., Graves, R.A., Budavari, A.I., Spiegelman, B.M., 1994a. mPPAR gamma 2: tissue-specific regulator of an adipocyte enhancer. Genes Dev. 8, 1224–1234.

Tontonoz, P., Hu, E., Spiegelman, B.M., 1994b. Stimulation of adipogenesis in fibroblasts by PPAR gamma 2, a lipid-activated transcription factor. Cell 79, 1147–1156.

Vidal-Puig, A.J., et al., 1997. Peroxisome proliferator-activated receptor gene expression in human tissues. Effects of obesity, weight loss, and regulation by insulin and glucocorticoids. J. Clin. Invest. 99, 2416–2422.

Wickham, T.J., et al., 1997. Increased in vitro and in vivo gene transfer by adenovirus vectors containing chimeric fiber proteins. J. Virol. 71, 8221–8229.

Wu, Z., Xie, Y., Morrison, R.F., Bucher, N.L., Farmer, S.R., 1998. PPAR gamma induces the insulin-dependent glucose transporter GLUT4 in the absence of C/EBPalpha during the conversion of 3T3 fibroblasts into adipocytes. J. Clin. Invest. 101, 22–32.

Yu, J.Y., DeRuiter, S.L., Turner, D.L., 2002. RNA interference by expression of short-interfering RNAs and hairpin RNAs in mammalian cells. Proc. Natl. Acad. Sci. U. S. A. 99, 6047–6052.

Zhao, L.J., Jian, H., Zhu, H., 2003. Specific gene inhibition by adenovirus-mediated expression of small interfering RNA. Gene 316, 137–141.

RESEARCH ARTICLE

Gene therapy for human small-cell lung carcinoma by inactivation of Skp-2 with virally mediated RNA interference

H Sumimoto[1], S Yamagata[1], A Shimizu[1], H Miyoshi[2], H Mizuguchi[3], T Hayakawa[4], M Miyagishi[5], K Taira[5] and Y Kawakami[1]

[1]Division of Cellular Signaling, Institute for Advanced Medical Research, Keio University School of Medicine, Shinjuku-ku, Tokyo, Japan; [2]Subteam for Manipulation of Cell Fate, BioResource Center, RIKEN Tsukuba Institute, Tsukuba, Japan; [3]Division of Cellular and Gene Therapy Products, National Institute of Health Sciences, Setagaya-ku, Tokyo, Japan; [4]National Institute of Health Sciences, Setagaya-ku, Tokyo, Japan; and [5]Department of Chemistry and Biotechnology, School of Engineering, The University of Tokyo, Hongo, Tokyo, Japan

Increase of Skp-2, which is involved in the degradation of cell cycle regulators including p27^{Kip1}, p21 and c-myc, is one of the important mechanisms for dysregulation of cell cycles in various cancers. We applied RNA interference (RNAi) for Skp-2 by using HIV-lentiviral or adenoviral vectors for a human small-cell lung carcinoma cell line with increased Skp-2 to evaluate RNAi strategy for cancer gene therapy. HIV-lentivirus-mediated RNAi for Skp-2 resulted in efficient inhibition of the in vitro cell growth of cancer cells with increased Skp-2 through the increase of p27^{Kip1} and p21, but no significant effect on the growth of cells without high Skp-2 expression. Furthermore, intratumoral administration of adenovirus siRNA vector for Skp-2 efficiently inhibited growth of established subcutaneous tumor on NOD/SCID mice. These results indicate that the Skp-2 RNAi may be a useful strategy for gene therapy of cancers with high Skp-2 expression.
Gene Therapy (2005) 12, 95–100. doi:10.1038/sj.gt.3302391
Published online 23 September 2004

Keywords: Skp-2; RNA interference; lentivirus; adenovirus

Introduction

Dysregulation of cell cycle is one of the important mechanisms for uncontrolled growth in most cancers. p27^{Kip1}, a cyclin-dependent kinase (cdk) inhibitor, inhibits the transition from G1 to S phase by suppressing the activity of a cyclin E/cdk2 complex in the late G1 to S phase.[1] In many cancers, including gastric, breast and colorectal cancers, low expression of p27^{Kip1} was reported to be associated with poor prognosis and highly aggressive nature of the tumors.[2] Since the level of the p27^{Kip1} protein is mainly controlled by ubiquitin–proteosomal proteolysis, enhanced degradation of p27^{Kip1} appeared to be an important mechanism for the reduction of p27^{Kip1} in cancers.[3] Skp-2, a member of the F-box protein family, is a specific substrate-recognition subunit of an SCF ubiquitin–protein ligase complex and is involved in the p27^{Kip1} degradation.[4] Increased expression of Skp-2, accompanied by inverse decrease of p27^{Kip1}, was reported in many cancers, including small-cell lung carcinoma (SCLC),[5] oral squamous cell carcinoma,[6] lymphoma[7] or gastric carcinoma,[2] indicating that Skp-2 may be involved in the tumorigenesis of some cancers with the reduced p27^{Kip1}. The Skp-2 was overexpressed in 44% of primary SCLC with the reduced expression of p27^{Kip1} through the gene amplification in 5p11–13.[5] Yokoi et al[5,8] have previously shown that downregulation of Skp-2 in an SCLC cell line with antisense oligonucleotides resulted in the inhibition of in vitro cell growth. However, the precise mechanism of growth inhibition by the Skp-2 inactivation remains to be investigated. In this study, we have analyzed the mechanism for the inhibition of tumor cell growth using newly developed HIV and adenoviral vectors expressing the Skp-2 siRNA, which may be useful for the future gene therapy.

Results

HIV vector-mediated RNA interference (RNAi) for Skp-2 resulted in the inhibition of in vitro cell growth of SCLC cell line with elevated Skp-2 expression

We constructed several HIV vectors expressing siRNAs targeting at the Skp-2 mRNA and analyzed their RNAi effects by determining the Skp-2 protein by Western blot analysis after infecting an SCLC cell line, ACC-LC-172, which has the gene amplification and increased expression of Skp-2. Of these siRNA HIV vectors, we selected two HIV vectors, S2 and S5, which mediated efficient reduction of the Skp-2 protein. We next evaluated effects of the RNAi for Skp-2 on in vitro growth of the ACC-LC-172 SCLC cells

by infection of these Skp-2 siRNA HIV vectors and a control siRNA HIV vector for firefly lucifrase (GL3B) whose infection did not affect *in vitro* growth, cell cycle status and amounts of Skp-2 protein of ACC-LC-172 compared to uninfected ACC-LC-172 (data not shown). *In vitro* cell growth of ACC-LC-172 was significantly inhibited when infected with the S5 siRNA HIV vector compared to the control GL3B siRNA HIV vector ($P < 0.0001$), although transduction efficiency monitored by GFP-expressing cells was comparable among the infected cells (98.7–99.9%). (Figure 1a). The similar cell growth inhibition was observed in a melanoma cell line, A375mel, with the overly expressed Skp2 (data not shown). *In vitro* growth of ACC-LC-172 infected with the S2 siRNA HIV vector was less inhibited than that with S5 ($P = 0.0005$) (Figure 1a), associated with the weaker suppression of Skp-2 and less induction of p27^{Kip1} and p21 compared to S5 (Figure 1b). The decrease of the Skp-2 protein accompanied by the reduction of p27^{Kip1} protein, shown by Western blot analysis of cell lysates at day 9 after the infection, was positively correlated with the inhibition of *in vitro* cell growth (Figure 1a and b). Other cdk inhibitor p21 was slightly elevated in the cells infected with the S2 and S5 siRNA HIV vectors similarly with p27^{Kip1} (Figure 1b). The p57^{Kip2} protein was under the detectable limit in this cell line (data not shown). The Rb protein was not changed after the infection. Cell cycle analysis performed on day 9 after the infection demonstrated decrease of the population in S and G2/M phases in the cells infected with the S5 siRNA HIV vector (44.6%) compared to those infected with the GL3B siRNA HIV vector (57.1%) (Table 1). No significant apoptosis was observed in the infected cells by flow cytometry analysis and DNA fragmentation assays (data not shown). These results indicated that the Skp-2 RNAi inhibited cellular growth of ACC-LC-172 through the increase of both cdk inhibitors p27^{Kip1} and p21. In contrast, *in vitro* growth of 293T cells without the Skp-2 overexpression was less sensitive to the inhibitory effect of the Skp-2 RNAi ($P = 0.1835$) (Figure 2a), although similar pattern of changes was observed in the Skp-2 and p27^{Kip1} proteins (Figure 2b). The constitutively low-level expression of the Skp-2 in 293T cells may explain the reason for the 293T resistance to the Skp-2 RNAi (Figure 2c). Similarly, *in vitro* cell growth of SBC-1, an SCLC cell line that lacks detectable Skp-2 expression, was not inhibited by the Skp-2 siRNAs (Figure 2d). Thus, virally mediated Skip2 RNAi does not appear to affect cells with low Skp2 expression.

Less involvement of myc in the inhibition of the ACC-LC-172 cell growth by the Skp-2 RNAi

Since Skp-2 was also reported to act as a transcriptional cofactor for c-myc,[9,10] which is involved in cell cycle progression by mediating the activation of cyclin E–cdk2 and cyclin D–cdk4, promoting the G1/S transition,[11] we evaluated the role of myc in the Skp-2 RNAi-mediated cell growth inhibition of the ACC-LC-172 SCLC cells. Increased myc expression was previously reported in most SCLC[11] and mild myc increase (2.03-fold) was detected in ACC-LC-172 (data not shown).

When a firefly luciferase expression plasmid, whose expression is under the control of human telomerase reverse transcriptase (hTERT) gene promoter containing
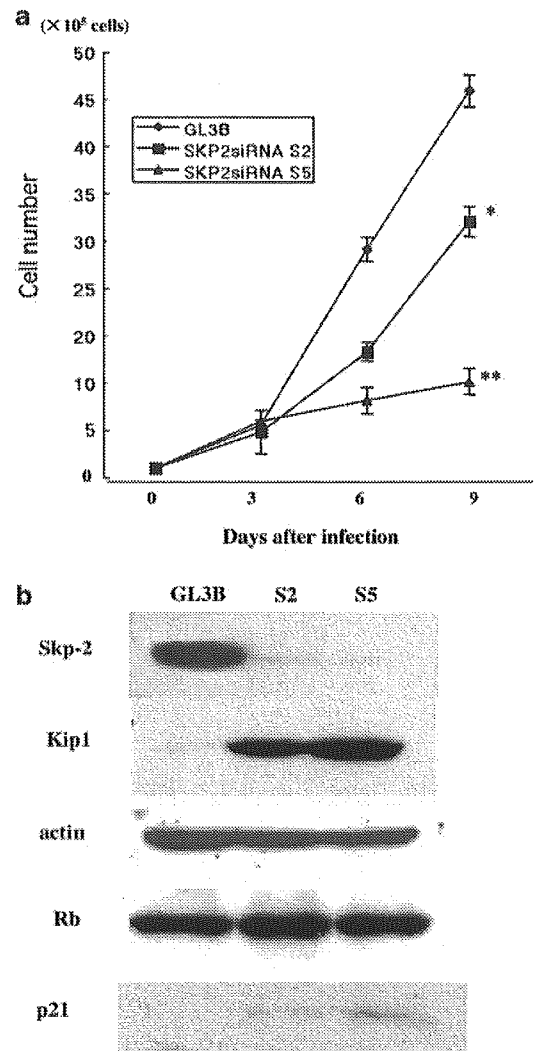

Figure 1 Inhibition of *in vitro* growth of an SCLC cell line along with decrease of Skp-2 and increase of p27^{Kip1} and p21 by infection of the HIV vectors expressing siRNA for Skp-2: (a) inhibition of *in vitro* tumor cell growth by virally medicated RNAi for Skp-2. SCLC cell line ACC-LC-172 (100 000) were infected with siRNA HIV vectors for control firefly luciferase (GL3B) or Skp-2 mRNA (S2 and S5) at 100 MOI on day 0, then the cell numbers were determined by trypan blue dye exclusion method on days 3, 6 and 9. The vertical bars indicate the s.d. of the triplicate assays (*$P = 0.0005$; **$P < 0.0001$). This is one representative result of three independent experiments with similar results. (b) Decrease of Skp-2 protein and increase of p27^{Kip1} and p21 proteins by virally medicated RNAi for Skp-2. Cell lysates were prepared from the cells infected with siRNA HIV vectors in (a) on day 9 after the infection. The Skp-2 protein was significantly decreased in cells infected with S2 and S5 compared to GL3B, and p27^{Kip1} and p21 proteins were reciprocally increased in cells infected with S2 and S5. The degrees of the increase of the p27^{Kip1} and p21 proteins were correlated with the degrees of the decrease of the Skp-2 protein. The transduction efficiency determined by GFP expression by flow cytometry was equivalent among the three groups (98.7–99.9%) at the harvest.

Table 1 Cell cycle status of ACC-LC-172 cells transduced with siRNA HIV vectors for firefly luciferase or Skp-2 mRNAs

siRNA	% G0/G1	% S	% G2/M
GL3B	42.92	45.40	11.68
S2	53.36	31.41	15.23
S5	55.39	35.38	9.23

two myc-binding E-box (CACGTG) motifs[12] (pGL3-hTERT), was transiently transfected to ACC-LC-172, the firefly luciferase activity normalized by *Renilla luciferase* activity was only minimally increased (1.1- to 2.7-fold) compared to that with a pGL3-Basic plasmid (Figure 3),
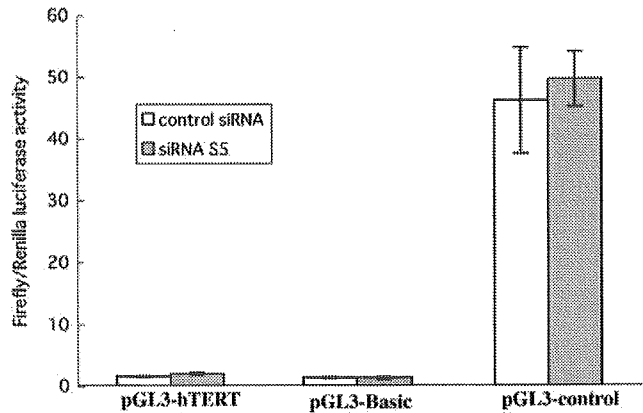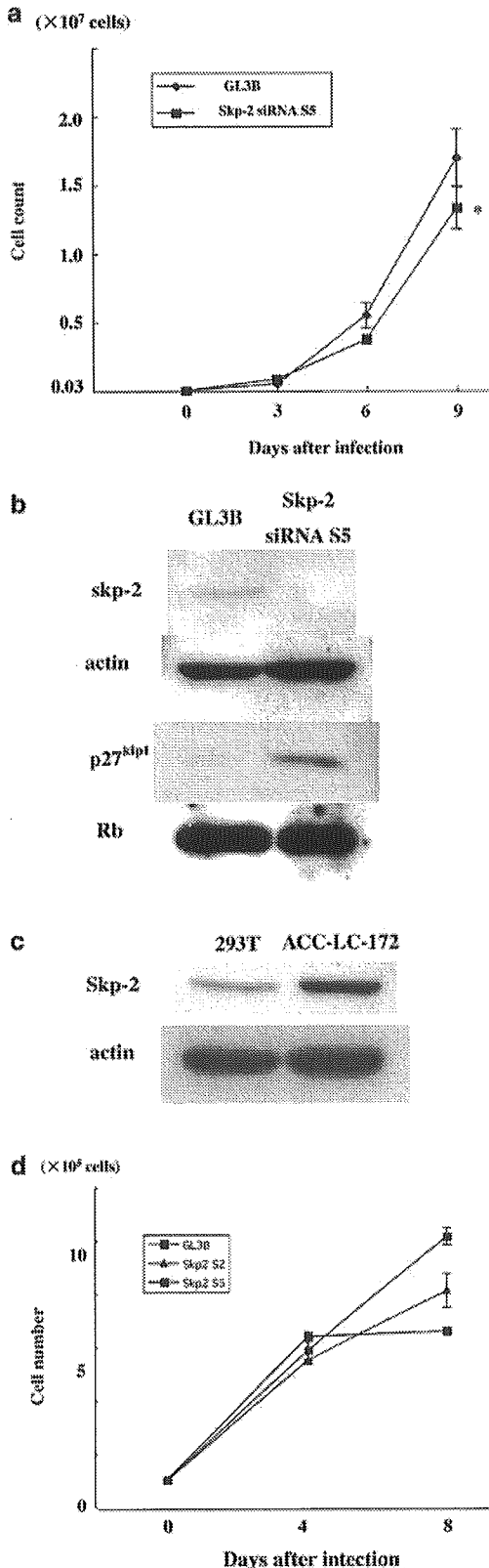
Figure 3 No involvement of myc in the Skp-2 RNAi-mediated cell growth inhibition in the ACC-LC-172 SCLC cell line: ACC-LC-172 cells stably expressing siRNA for Skp-2 (siRNA S5) or control siRNA were transfected with 1 μg of pRL-SV40 (Renilla luciferase expressing plasmid) and 1 μg of pGL3-hTERT, pGL3-Basic or pGL3-control (firefly luciferase expressing plasmids driven by different promoters) by using lipofectamine. At 48 h after the transfection, the cells were harvested and the both Renilla and firefly luciferase activities were determined. Each firefly luciferase activity normalized by the Renilla luciferase activity was calculated. The normalized firefly luciferase activity with pGL3-hTERT was minimally elevated by 1.6-fold compared to with pGL3-Basic without any inhibition in the presence of siRNA for Skp-2. Each bar represents the mean value of triplicate assays and error bars represent the s.d. This is one representative result of three independent experiments with similar results.

suggesting that constitutive myc activity was relatively low in the ACC-LC-172 cells. Transfection of the same plasmid into the ACC-LC-172 cells stably transduced with the HIV Skp-2 siRNA vector (siRNA S5) did not change the luciferase activity. These results indicated that enhancement of myc activity was not the mechanism for the cell growth inhibition of ACC-LC-172 by the Skp-2 RNAi.

In vivo therapeutic activity of intratumoral administration of adenovirus siRNA for Skp-2

To evaluate therapeutic ability of the RNAi for Skp-2, we constructed an adenovirus vector expressing siRNA for

Figure 2 Minimal inhibition of in vitro growth of 293T cells without increase of Skp-2 expression by infection of the Skp-2 siRNA HIV vectors: minimal inhibition of in vitro growth of 293T cells by the Skp-2 siRNA HIV vector infection. The 293T cells (30 000) were infected with siRNA HIV vectors for control GL3B or Skp-2 mRNA (S5) at 100 MOI on day 0, then the cell numbers were determined as Figure 1a. The vertical bars indicate the s.d. of the triplicate assays (*P = 0.1835). This is one representative result of three independent experiments with similar results. (b) Decrease of the Skp-2 protein and increase of the p27Kip1 protein by the Skp-2 siRNA HIV vector infection. Cell lysates were prepared as in Figure 1b. Relatively low expression Skp-2 protein was decreased in cells infected with S5 compared to GL3B, and the p27Kip1 protein was reciprocally increased in cells infected with S5, although the changes were less prominent than observed in ACC-LC172 cells. The transduction efficiency determined by GFP expression by flow cytometry was equivalent between the two groups (GL3B: 95.4%; S5: 100.0%) at the harvest. (c) Low expression of Skp-2 in 293T cells compared to ACC-LC-172 SCLC cell line. The amount of the Skp-2 protein was much lower in 293T cells than in ACC-LC-172 cells. The percentage of S+G2/M populations in 293T cells and ACC-LC-172 cells was 74.0 and 58.4%, respectively, at the harvest. (d) SBC-1 SCLC cells lacking detectable Skp-2 were refractory to Skp-2 RNAi. The in vitro cell growth of SBC-1, an SCLC cell line without detectable Skp-2 protein, was not inhibited with Skp-2 siRNA vectors.

Skp-2, AdF35-Skp-2 siRNA S5, since adenovirus vector is more effective for *in vivo* gene transfer with more efficient production of high-titer viruses. The constructed adenovirus reduced the Skp-2 protein very efficiently in the ACC-LC-172 SCLC cells at only 5 multiplicity of infection (MOI) (Figure 4a), and inhibited the cell growth compared with the control AdF35-GL3B (data not shown). When these adenoviruses were intra-tumorally injected three times every 2 days to subcutaneously grown ACC-LC-172 SCLC tumors with the largest diameter of 3–4 mm on immunodeficient NOD/SCID mice, growth of tumors injected with the AdF35-Skp-2 siRNA (S5) was significantly reduced compared to that with the control AdF35-GL3B ($P < 0.05$) (Figure 4b). These results indicated that Skp-2 is an excellent target for the treatment of cancers with the increased Skp-2, and gene therapy by virally mediated RNAi may be applicable for these cancers.
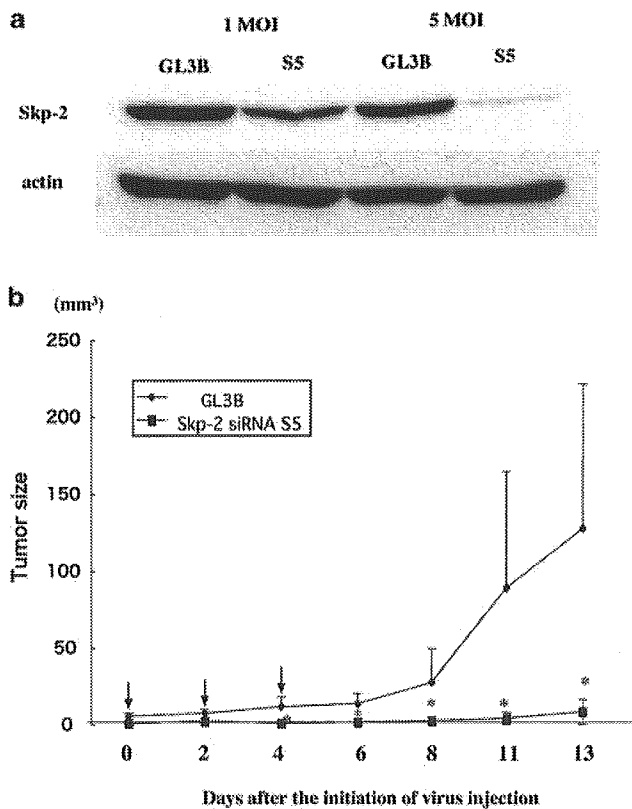

Figure 4 Inhibition of in vivo tumor growth by intratumoral administration of adenoviral vector expressing siRNA for Skp-2. (a) Efficient downregulation of Skp-2 protein by infection of the Skp-2 siRNA adenoviral vector. Cell lysates from ACC-LC-172 cells infected with AdF35-Skp-2 siRNA S5 or AdF35-GL3B at either 1 or 5 MOI were prepared and analyzed for Skp-2 protein by Western blot analysis. (b) Inhibition of in vivo tumor growth by intratumoral injection of the Skp-2 siRNA. A total of 1×10^8 IFU of AdF35-Skp-2 siRNA S5 (n = 5) or AdF35-GL3B (control) (n = 4) were intratumorally injected three times every 2 days as shown in the figure (arrow) to subcutaneously established ACC-LC-172 on NOD/SCID mice. The largest diameter of the tumor reached 3–4 mm when injected with adenoviral vectors. The tumor size was compared between the two groups. *P < 0.05, the vertical bars indicate s.d.

Discussion

The cdk inhibitor, p27[Kip1], controls progression of cell cycles in response to mitogenic stimuli, and is a dosage-dependent tumor suppressor protein.[3] Reduced expression of p27[Kip1] is not usually caused by genetic change,[3] but often caused by enhanced proteolysis in cancers. The targeted disruption of an ubiquitin–protein ligase Skp-2 resulted in cell cycle arrest in G1 with the accumulation of p27[Kip1],[13] indicating that Skp-2 regulate cell cycle progression through proteolysis of p27[Kip1]. Patients with cancers with the reduced p27[Kip1] by increased expression of Skp-2 were reported to have relatively poor prognosis in clinical studies.[6–8]

In this study, we attempted virally mediated RNAi for Skp-2 on the SCLC cell line to analyze the role of Skp-2 in the cell growth as well as to develop possible gene therapy for the Skp-2 overexpressing cancers. The observation that cell growth was inhibited by the virally mediated Skp-2 RNAi, which was accompanied by downregulation of Skp-2 and upregulation of both p27[Kip1] and p21, indicated that the increased Skp-2 expression is a primary event causing cell cycle progression of the SCLC cell line through the enhanced proteolytic degradation of p27[Kip1]. Interestingly, the degree of the Skp-2 suppression with different siRNAs was correlated with the degree of the elevation of p27[Kip1] and p21 as well as *in vitro* growth suppression. Although p21 is mainly regulated transcriptionally, Skp-2-mediated ubiquitination and the subsequent proteolysis appear to be involved in the regulation of p21.[14] Although the increase of p21 was not as prominent as that of p27[Kip1], we also observed significant increase of p21 after the Skp-2 RNAi, indicating that it may also contribute to the cell cycle progression in the SCLC cell line.

Although Yokoi *et al* reported that antisense oligonucleotide-mediated inactivation of Skp-2 resulted in the induction of apoptosis characterized by an increase of the sub-G1 population, fragmentation of nuclei and activation of caspase-3 when evaluated on days 2–4,[8] we did not observe significant increase of the sub-G1 population or DNA fragmentation in the ACC-LC-172 cells with the siRNA HIV vectors in spite of very efficient downregulation of Skp-2 on day 9 (data not shown). This discrepancy may result from the different time point. Remaining on day 9 after the lentiviral infection cells might have been refractory to the apoptotis.

In contrast to the previous reports using Skp-2$^{-/-}$ mice[13] or forced expression of p27[Kip1],[1] Skp-2 RNAi did not lead to complete G1 arrest. Although almost complete downregulation of the Skp-2 protein accompanied by the increase of the p27[Kip1] protein was observed with the siRNA S5 (Figure 1b), these infected cells continued to grow slowly (Figure 1a), possibly due to relative resistance of this cell line to cell cycle inhibition by p27[Kip1].

In terms of possible use of this strategy for treatment of cancer patients, along with the effective tumor growth inhibition, it should be noted that growth of cells without the increased Skp-2, including 293T cells and primary fibroblasts (data not shown) was hardly affected by Skp-2 RNAi, suggesting that inactivation of Skp-2 is a relatively safe targeting therapy for cancers with high Skp-2 expression. In this study, we also demonstrated

that intratumoral injection of adenovirus vector expressing the Skp-2 siRNA efficiently inhibited *in vivo* growth of the established tumor subcutaneously implanted in NOD/SCID mice, suggesting that viral-mediated Skp-2 RNAi may be applicable for gene therapy. These results altogether indicated that Skp-2 is a good target for gene therapy or other molecular target therapy for patients with cancers expressing high level of Skp-2.

Materials and methods

Cell lines

An ACC-LC-172 cell line (a kind gift from Dr Takahashi, Aichi Cancer Center, Research Institute, Japan) and SBC-1 (purchased from Japanese Collection of Research Bioresources, Japan) established from Japanese patients with SCLC were maintained in RPMI-1640 (Sigma, Japan) supplemented with 10% (v/v) fetal bovine serum, penicillin and streptomycin. The 293T cells were purchased from American Type Culture Collection (ATCC, Manassas, VA, USA) and maintained in DMEM (Sigma, Japan) supplemented with 10% (v/v) fetal bovine serum, penicillin and streptomycin.

HIV vectors

HIV vectors for siRNA expression were constructed from an HIV-U6i-GFP plasmid, which was described previously.[15,16] Briefly, HIV-U6i-GFP has two expression units: one was an siRNA expression cassette, from which a short hairpin RNA was transcribed from human U6 promoter, and the second was a GFP expression cassette, from which GFP gene was transcribed from the CMV promoter. For siRNA expression, *in vitro* annealed complementary oligonucleotides for target sequences were inserted into the two *Bsp*MI sites downstream of the human U6 promoter. Two siRNA target sequences were selected for the Skp-2 RNAi: (S2) ATCA GATCTCTCTACTTTA and (S5) AGGTCTCTGGTGTTT GTAA. Two complementary oligonucleotides, cacc-(target sense)-TTCAAGAGA-(target antisense)-TTTTT and gcatAAAAA-(target sense)-TCTCTTGAA-(target antisense) were synthesized for each target sequence and annealed *in vitro*. The annealed double-stranded (ds) oligonucleotides with 5′-protruding ends complementary to the two *Bsp*MI sites in the HIV-U6i-GFP plasmid were then subcloned into the HIV-U6i-GFP. Control GL3B siRNA (anti-firefly luciferase siRNA) HIV vector was also constructed with the target sequence GTGCGCTGCTGGTGCCAAC. A mutation-specific anti-BRAF siRNA HIV vector (target: GCTACAGA GAAATCTCGATGG) was used for control in a reporter assay. These HIV vectors produce a short hairpin RNA with the linker sequence (TTCAAGAGA) forming a loop structure, then the linker is processed by Dicer, forming a dsRNA that act as an siRNA. The third-generation HIV vectors were produced by transfecting 293T cells with HIV plasmid vectors, pMD.G (VSV-G env expression plasmid), pMDLg/p.RRE (the third-generation packaging plasmid) and pRSV Rev (Rev expression plasmid) (the latter two plasmids were provided by Cell Genesys, USA) by calcium phosphate transfection. The culture supernatants were collected and used as virus stocks after concentration. The viral titer was measured by counting GFP-positive cells after infection on 293T cells.

In vitro growth inhibition assay

ACC-LC-172 cells (100 000) were infected with the siRNA HIV vectors for Skp-2 (S2 or S5) or firefly luciferase (GL3B) at 100 MOI at day 0. Cell numbers were counted every 3 days by trypan blue dye exclusion method until day 9. The 293T cells (30 000) were infected with siRNA HIV vectors for control GL3B or Skp-2 (S5) at 100 MOI at day 0, then the cell numbers were determined every 3 days until day 9. SBC-1 cells (100 000) were infected with the siRNA HIV vectors, S2, S5 or GL3B at 100 MOI. Cell numbers were counted every 4 days until day 8.

Western blot analysis

Cell lysates were prepared in the lysis buffer (20 mM Tris-HCl (pH 7.5), 12.5 mM β-glycerophosphate, 2 mM EGTA, 10 mM NaF, 1 mM benzamide, 1% NP-40, protease inhibition cocktail (complete, EDTA-free (Roche, Germany)) and 1 mM Na_3VO_4) from the infected cells used in *in vitro* growth inhibition assay on day 9 after confirmation of equivalent GFP expression among the groups by flow cytometry. The protein concentration was determined by DC protein assay kit (Bio-Rad, USA). Anti-p45^{Skp-2} (Zymed Laboratories Inc., CA, USA), anti-actin (Sigma, USA), anti-p27^{Kip1} (BD Transduction, USA), anti-Rb (Cell Signaling, USA) or anti-p21 (Santa Cruz, USA) Abs was used for the first antibody. An HRP-conjugated anti-IgG antibody was used for the second antibody, and the reaction was detected by chemiluminescence with SuperSignal West Femto Maximum Sensitivity Substrate (Pierce, USA).

Cell cycle analysis

The cells used in the *in vitro* growth inhibition assays were harvested on day 9 and stained with propidium iodide (PI) by using CycleTEST PLUS DNA Reagent Kit (Becton Dickinson, San Jose, CA, USA) according to the manufacturer's instruction. After the stained cells were analyzed by FACSCalibur (Becton Dickinson), the cell cycle status was analyzed with ModFit software (Becton Dickinson).

hTERT reporter construction

A 0.4 kb hTERT promoter sequence was amplified by genomic PCR with the forward primer: CGCTGG GGCCCTCGC TGGCGTCCCT (nts −324 to −300, numbered relative to the translation initiation site); and the reverse primer: CAGCGGCAGCACCTCGCGGTAGTGG (nts +48 to +72). After denaturation for 4 min at 95°C, 27 cycles of denaturation for 1 min at 95°C, annealing for 1 min at 70°C and extension for 1 min at 72°C were performed and followed by completion for 7 min at 72°C. The PCR product was subcloned into a pCRII vector of TA Cloning kit (Invitrogen, San Diego, CA). After the confirmation of the correct sequence, the translation initiation codon was mutated from ATG to TTG by using QuikChange site-directed mutagenesis kit (STRATA-GENE, La Jolla, CA, USA). Then, the hTERT promoter was subcloned into a pGL3-Basic vector (Promega, Madison, WI, USA). The resultant construct, pGL3-hTERT, transcribes the firefly luciferase gene under the control of the 0.4 kb hTERT promoter.

Reporter assay

ACC-LC-172 cells (500 000) stably expressing siRNA for Skp-2 (S5) or for BRAF (V599E) (control siRNA specific

100

for mutated BRAF (V599E) after the infection with HIV vectors) were transfected with 1 µg of *Renilla luciferase* expression plasmid, pRL-SV40 (Promega) and 1 µg of one of the following firefly luciferase expression plasmids: pGL3-hTERT, pGL3-Basic or pGL3-control (Promega) by using Lipofectamine (Invitrogen). At 48 h after the transfection, the cells were harvested and the luciferase activity was analyzed using Dual-Glo Luciferase Assay System (Promega) and a Berthold luminometer. Each firefly luciferase activity was normalized to *Renilla luciferase* activity.

Adenovirus vectors for siRNA

The adenovirus vectors containing Ad5/35 chimeric fiber protein[17] were used in this study. The vector plasmids pAdF35 and the shuttle vector plasmid pHMCMV-GFP1 were described previously.[18] pHMCMV-GFP1 contains the CMV promoter, the GFP gene derived from pEGFP-N1 (Clontech, Palo Alto, CA, USA) and the bovine growth hormone (BGH) poly(A) signal. The siRNA expression unit containing human U6 promoter and two *Bsp*MI cloning sites were excised from the HIV-U6i-GFP plasmid by *Eco*RI digestion, then subcloned into the *Eco*RI site in pHMCMV-GFP1, which was located downstream of the BGH poly(A) signal. This vector was designated as pHMCMV-GFP-U6i. The ds oligonucleotides for the short hairpin RNA can be directly subcloned into the two *Bsp*MI sites of the pHMCMV-GFP-U6i as in HIV-U6i-GFP. Accordingly, the shuttle vector plasmids containing ds oligonucleotides for Skp-2 (S5) or GL3B were constructed. The adenovirus vectors, AdF35-Skp-2 siRNA S5 and AdF35-GL3B, were constructed by an improved *in vitro* ligation method as described.[19] Both adenovirus vectors were propagated in 293 cells and the viral titers were determined using Adeno-X Rpaid Titer Kit (Clontech) according to the manufacturer's instructions.

Animal experiments

Male NOD/SCID mice (6 weeks old) (Japan Clea, Japan) were subcutaneously implanted with 5×10^6 ACC-LC-172 cells. About 1 week after the implantation, when the largest tumor diameter reached about 3–4 mm, we injected 1×10^8 IFU of AdF35-Skp-2 siRNA S5 or AdF35-GL3B into the tumor (day 0). The adenovirus injection was repeated twice every 2 days. The tumor volume (the largest diameter × the perpendicular diameter × the height) was measured every 2 or 3 days until day 13. The animal experimental protocol was approved by the Laboratory Animal Care and Use Committee at Keio University School of Medicine. Mice were treated according to the Guidelines for the Care and Use of Laboratory Animals of Keio University School of Medicine.

Statistical analysis

All statistical analyses were performed according to unpaired Student's *t*-test.

Acknowledgements

References

1 Toyoshima H, Hunter T. p27, a novel inhibitor of G1 cyclin–Cdk protein kinase activity, is related to p21. *Cell* 1994; **78**: 67–74.

2 Masuda T *et al.* Clinical and biological significance of S-phase kinase-associated protein 2 (Skp2) gene expression in gastric carcinoma: modulation of malignant phenotype by Skp2 overexpression, possibly via p27 proteolysis. *Cancer Res* 2002; **62**: 3819–3825.

3 Fero ML *et al.* The murine gene p27Kip1 is haplo-insufficient for tumor progression. *Nature* 1998; **396**: 177–180.

4 Sutterlüty H *et al.* p45SKP2 promotes p27Kip1 degradation and induces S phase in quiescent cells. *Nat Cell Biol* 1999; **1**: 207–214.

5 Yokoi S *et al.* A novel target gene, SKP2, within the 5p13 amplicon that is frequently detected in small cell lung cancers. *Am J Pathol* 2002; **161**: 207–216.

6 Gstaiger M *et al.* Skp2 is oncogenic and overexpressed in human cancers. *Proc Natl Acad Sci USA* 2001; **98**: 5043–5048.

7 Latres E *et al.* Role of the F-box protein Skp-2 in lymphomagenesis. *Proc Natl Acad Sci USA* 2001; **98**: 2515–2520.

8 Yokoi S *et al.* Down-regulation of SKP2 induces apoptosis in lung-cancer cells. *Cancer Sci* 2003; **94**: 344–349.

9 Kim SY *et al.* Skp2 regulates myc protein stability and activity. *Mol Cell* 2003; **11**: 1177–1188.

10 Lehr N *et al.* The F-box protein Skp2 participates in c-myc proteosomal degradation and acts as a cofactor for c-myc-regulated transcription. *Mol Cell* 2003; **11**: 1189–1200.

11 Zajac-Kaye M. Myc oncogene: a key component in cell cycle regulation and its implication for lung cancer. *Lung Cancer* 2001; **34**: S43–S46.

12 Greenberg RA *et al.* Telomerase reverse transcriptase gene is a direct target of c-Myc but is not functionally equivalent in cellular transformation. *Oncogene* 1999; **18**: 1219–1226.

13 Nakayama K *et al.* Targeted disruption of Skp2 results in accumulation of cyclin E and p27Kip1, polyploidy and centrosome overduplication. *EMBO J* 2000; **19**: 2069–2081.

14 Bornstein G *et al.* Role of the SCFSkp2 ubiquitin ligase in the degradation of p21Cip1 in S phase. *J Biol Chem* 2003; **278**: 25752–25757.

15 Miyagishi M *et al.* Optimization of an siRNA-expression system with an improved hairpin and its significant suppressive effects in mammalian cells. *J Gene Med* 2004; **6**: 715–723.

16 Sumimoto H *et al.* Inhibition of growth and invasive ability of melanoma by inactivation of mutated BRAF with lentivirus-mediated RNA interference. *Oncogene* 2004; **23**: 6031–6039.

17 Mizuguchi H, Hayakawa T. Adenovirus vectors containing chimeric type 5 and type 35 fiber proteins exhibit altered and expanded tropism and increase the size limit of foreign genes. *Gene* 2002; **285**: 69–77.

18 Okada N *et al.* Efficient antigen gene transduction using Arg-Gly-Asp fiber-mutant adenovirus vectors can potentiate anti-tumor vaccine efficacy and maturation of murine dendritic cells. *Cancer Res* 2001; **61**: 7913–7919.

19 Mizuguchi H, Kay MA. Efficient construction of a recombinant adenovirus vector by an improved *in vitro* ligation method. *Hum Gene Ther* 1998; **9**: 2577–2583.

RESEARCH ARTICLE

Augmentation of the migratory ability of DC-based vaccine into regional lymph nodes by efficient CCR7 gene transduction

N Okada[1], N Mori[1], R Koretomo[1], Y Okada[2], T Nakayama[3], O Yoshie[3], H Mizuguchi[4], T Hayakawa[5], S Nakagawa[6], T Mayumi[6], T Fujita[1] and A Yamamoto[1]

[1]Department of Biopharmaceutics, Kyoto Pharmaceutical University, Misasagi, Yamashina-ku, Kyoto, Japan; [2]Research Institute for Microbial Diseases, Osaka University, Osaka, Japan; [3]Department of Microbiology, Kinki University School of Medicine, Osaka-Sayama, Osaka, Japan; [4]Division of Cellular and Gene Therapy Products, National Institute of Health Sciences, Setagaya-ku, Tokyo, Japan; [5]National Institute of Health Sciences, Setagaya-ku, Tokyo, Japan; and [6]Department of Biopharmaceutics, Graduate School of Pharmaceutical Sciences, Osaka University, Osaka, Japan

Although dendritic cell (DC)-based immunotherapy is considered a promising approach for cancer treatment, a large quantity of DC vaccine is required for effective sensitization/activation of immune cells because of the poor migratory ability of administered DCs into regional lymphoid tissue. In this study, we created a DC vaccine sufficiently transduced with CC chemokine receptor-7 gene (CCR7/DCs) by applying RGD fiber-mutant adenovirus vector (AdRGD), and investigated its immunological characteristics and therapeutic efficacy. CCR7/DCs acquired strong chemotactic activity for CC chemokine ligand-21 (CCL21) and exhibited an immunophenotype similar to mature DCs but not immature DCs with regard to major histocompatibility complex/costimulatory molecule-expression levels and allogenic T cell proliferation-stimulating ability, while maintaining inherent endocytotic activity. Importantly, CCR7/DCs injected intradermally into mice could accumulate in draining lymph nodes about 5.5-fold more efficiently than control AdRGD-applied DCs. Reflecting these properties of CCR7/DCs, DC vaccine genetically engineered to simultaneously express endogenous antigen and CCR7 could elicit more effective antigen-specific immune response in vivo using a lower dosage than DC vaccine transduced with antigen alone. Therefore, the application of CCR7/DCs having positive migratory ability to lymphoid tissues may contribute to reduction of efforts and costs associated with DC vaccine preparation by considerably reducing the DC vaccine dosage needed to achieve effective treatment by DC-based immunotherapy.
Gene Therapy (2005) 12, 129–139. doi:10.1038/sj.gt.3302358
Published online 14 October 2004

Keywords: dendritic cell-based vaccination; RGD fiber-mutant adenovirus vector; CCR7; migration; melanoma

Introduction

Immunotherapy using dendritic cells (DCs), which play a critical role in control of both acquired and innate immune responses in the living body, is studied energetically in many research organizations aiming to immunologically eradicate cancer. In addition, several cancer immunotherapy protocols using DC vaccine introduced with tumor-associated antigen (TAA) advanced to the clinical study phase.[1–4] However, since currently available DC-based immunotherapy has not demonstrated exceptional therapeutic effects in these clinical studies, the development of a novel approach capable of improving the efficacy of this promising strategy for cancer treatment is eagerly awaited.

DCs are widely distributed over peripheral tissues, where they catch invading antigens by full endocytotic activity, characteristic of an immature state. The pheno-type of DCs internalizing antigens changes to a mature state in response to these inflammatory stimuli. Subsequently, they process the antigens into the peptides presented on major histocompatibility complex (MHC) molecules, migrate into draining lymph nodes (LNs) via afferent lymphatic venules, and induce primary immune responses through antigen presentation to T cells.[5–7] On the basis of these serial immune mechanisms, the degree of administered DC vaccine accumulation in lymphoid tissues is a factor in enhancing or restricting therapeutic effects in DC-based immunotherapy.

In recent years, identification and functional analysis of chemokines/chemokine receptors, which regulate relevant leukocyte migration and invasion into tissues, have progressed remarkably, and the chemokine–chemokine receptor coupling in DC migration from peripheral tissue to lymphoid tissue has been elucidated. Gunn et al[8] found that DC migration to secondary lymphoid tissues was inhibited in CC chemokine ligand-21 (CCL21) expression-defective plt/plt mice. Likewise, Förster et al[9] reported that inhibition of DC migration to secondary lymphoid tissues occurred in CC chemokine receptor-7 (CCR7)-knockout mice. Based on these results, the association between CCL21, which is pro-

duced and secreted constitutively in lymphoid tissues and lymphatic vessels, and CCR7, a seven-transmembrane domain G-protein-coupled receptor whose expression is enhanced on the surface of maturing DCs, has been shown to play a central role in control of DC migration from the peripheral tissue to lymphoid tissues. Therefore, DCs, which are not only introduced with antigens but also exhibit enhanced CCR7 expression, may positively migrate to lymphoid tissue and efficiently activate the host's immune system after administration to a living body. Efficient CCR7-gene transduction to DCs is proposed as a preparatory method for this novel 'lymphoid tissue-directivity DC' vaccine.

Efficient gene transduction to DCs is difficult in any conventional vector system including adenovirus vector (Ad), which could transfect in a wide variety of cells and tissues.[10] In this regard, we succeeded in establishing highly efficient gene transduction to DCs by applying RGD fiber-mutant Ad (AdRGD),[11-14] and clarified that vaccination with DCs transduced with TAA gene using AdRGD induced considerable antitumor effect based on activation of TAA-specific cytotoxic T lymphocytes (CTLs) in mice.[12,14] Our results not only revealed that AdRGD is very useful in antigen gene delivery to DCs, but also opened up new potentiality for genetically enhancing the immunological functions of DCs by

making use of the predominance of AdRGD in gene transduction efficiency to DCs. Thus, in the present study, we first constructed an AdRGD-carrying CCR7 gene (AdRGD-CCR7), and investigated the immunological properties and vaccine efficacy of murine bone marrow-derived DCs modified with AdRGD-CCR7 in order to create a 'lymphoid tissue-directivity DC' vaccine.

Results

Gene transduction into DCs by AdRGD-CCR7

We examined the cytopathic effects of gene transduction using AdRGD-CCR7 to DCs by MTT assay. AdRGD-CCR7 did not injure DCs with a vector dose of 100 multiplicities of infection (MOI) or less, whereas viability of DCs was slightly reduced by using AdRGD-CCR7 at 200 MOI (data not shown). Thus, CCR7 gene expression was evaluated by semiquantitative reverse transcription-polymerase chain reaction (RT-PCR) analysis in DCs transduced with AdRGD-CCR7 at 100 MOI or less. The CCR7 mRNA level of lipopolysaccharide-stimulated DCs (LPS/DCs) or Luc/DCs transduced with AdRGD-Luc (luciferase-expressing control vector) at 50 MOI did not show a remarkable change in comparison with that of mock (immature) DCs at 24 h post-treatment (Figure 1a).
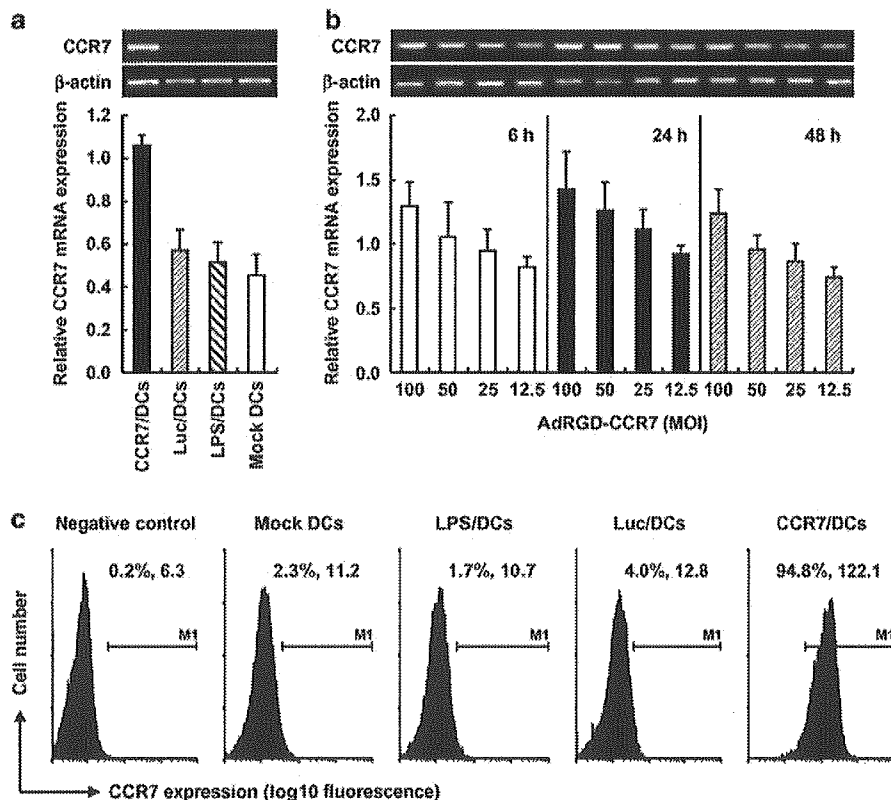

Figure 1 RT-PCR and flow cytometric analysis for mouse CCR7 expression levels. DCs were transduced with AdRGD-CCR7 or AdRGD-Luc at 50 MOI (a and c) or the indicated MOI (b). These transduced cells, LPS-stimulated DCs, and mock DCs were cultured for 24 h (a and c) or the indicated period (b) in GM-CSF-free medium. (a and b) Total RNA was isolated from these DCs, and then mouse CCR7 mRNA expression was assessed by RT-PCR analysis. Relative CCR7 mRNA expression was calculated as ratio of the densitometric units of PCR products derived from CCR7 transcripts to the densitometric units of PCR products derived from β-actin transcripts. Data are presented as mean±s.d. of results from three independent experiments. (c) Flow cytometric analysis was performed by using anti-mouse CCR7 antibody. Negative control represents mock DCs stained by second antibody alone. The data are representative of two independent experiments, and the % value and the numerical value indicated in the upper part of each panel express % of M1-gated cells and mean fluorescence intensity (MFI), respectively.

On the other hand, CCR7/DCs prepared with AdRGD-CCR7 at 50 MOI were able to express CCR7 mRNA at a level more than double that of mock DCs. In addition, we analyzed the changes in CCR7 mRNA expression over time in CCR7/DCs transduced at various vector doses (Figure 1b). It was revealed that CCR7 mRNA expression in CCR7/DCs increased in a vector dose-dependent manner, and highest levels were observed at 24 h after gene transduction. Moreover, flow cytometric analysis using anti-mouse CCR7 polyclonal antibody showed that most of the CCR7/DCs, which were prepared with AdRGD-CCR7 at 50 MOI and then cultured for 24 h, expressed CCR7 protein on their surface, whereas few CCR7-positive cells were detected in mock DCs, LPS/DCs, and Luc/DCs (Figure 1c).

Next, we evaluated the chemotactic activity of CCR7/DCs for CCL21 by in vitro chemotaxis assay in order to confirm functional CCR7 expression on the cell surface. Under transductional conditions at an MOI of 50, the number of migrating CCR7/DCs cultured for 24 h markedly increased with increasing CCL21 concentration, whereas Luc/DCs, LPS/DCs, and mock DCs remained at low levels despite CCL21 stimulation (Figure 2a). Furthermore, as was observed for RT-PCR analysis in Figure 1b, the chemotactic activity of CCR7/DCs for CCL21 was enhanced with increasing AdRGD-CCR7 dose during transduction (Figure 2b). These results clearly demonstrated that functional CCR7, which could promote migration of DCs in response to a CCL21 concentration gradient, was expressed on the CCR7/DC surface, and that transduction of the chemokine receptor gene by AdRGD could modify chemokine responsiveness of DCs.

Immunological properties of CCR7/DCs

We analyzed the immunological characteristics of CCR7/DCs prepared with AdRGD-CCR7 at 50 MOI. At first, the expression levels of MHC/costimulatory molecules in CCR7/DCs cultured for 24 h were analyzed by flow cytometry (Figure 3a). In comparison with mock DCs, CCR7/DCs and Luc/DCs exhibited upregulated expression of all tested surface marker molecules, which play critical roles in the sensitization/activation of T cells, as is seen in mature LPS/DCs. In particular, the expression levels of CD40 and CD86 were dramatically enhanced by gene transduction using AdRGD. This result agreed with our previous report demonstrating that transduction using AdRGD, irrespective of the type of inserted transgene, could enhance the expression of MHC/costimulatory molecules on DCs.[13] Moreover, CCR7/DCs were able to stimulate proliferation of allogenic naive T cells in mixed leukocyte reaction (MLR) more effectively than mock DCs, and the stimulatory ability of CCR7/DCs, Luc/DCs, and LPS/DCs was equal at a responder/stimulator ratio of 5 (Figure 3b).

The level of fluorescein isothiocyanate (FITC)-dextran uptake in CCR7/DCs was estimated as an index of their endocytotic activity (Figure 3c). Excellent endocytosis for FITC-dextran was observed in mock DCs incubated at 37°C, whereas fluorescence intensity derived from internalized FITC-dextran was drastically decreased by 4°C incubation or LPS-driving maturation. On the other hand, FITC-dextran-uptake levels in CCR7/DCs and Luc/DCs, which were cultured for 24 h after gene transduction, were comparable to those in mock DCs.
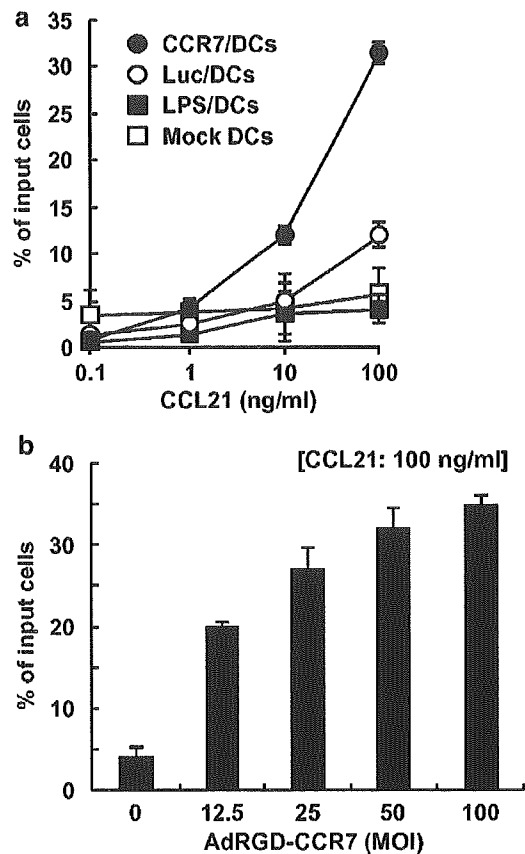

Figure 2 Chemotactic activity of CCR7/DCs in response to CCL21. DCs were transduced with AdRGD-CCR7 or AdRGD-Luc at 50 MOI (a) or the indicated MOI (b). These transduced cells, LPS-stimulated DCs, and mock DCs were cultured for 24 h in GM-CSF-free medium. In vitro chemotaxis assay was performed by a Chemotaxicell-24 installed on a 24-well culture plate. CCL21 solution was added in the lower compartment at the indicated concentration, and DCs were placed in the upper chamber at 10^6 cells. After 4 h incubation, the number of cells that migrated to the lower compartment was counted on a NucleoCounter. Data are presented as mean ± s.d. of four independent cultures.

Taken together, these results demonstrate that gene transduction using AdRGD-CCR7 did not eliminate the antigen-presenting cell (APC) function of DCs; rather, CCR7/DCs acquired an immunophenotype similar to mature DCs while maintaining high endocytotic capacity. Additionally, these immunological characteristics of CCR7/DCs were similar at 48 h post-transduction (data not shown).

Accumulation of CCR7/DCs in regional LN

DCs derived from enhanced green fluorescent protein-transgenic (EGFP-Tg) mice were transduced with AdRGD-CCR7 or AdRGD-Luc at 50 MOI and then cultured for 24 h. These EGFP-positive CCR7/DCs, Luc/DCs, and mock DCs were intradermally injected into the flank of wild-type mice, and their accumulation in the draining inguinal LN was compared at 48 h post-administration by flow cytometric analysis (Figure 4). In all mice, the EGFP-positive DCs were not detected in the inguinal LNs contralateral to the DC-administration site (data not shown). More than double the number of EGFP-positive DCs was detected in regional LN cells prepared from mice injected with Luc/DCs, as compared
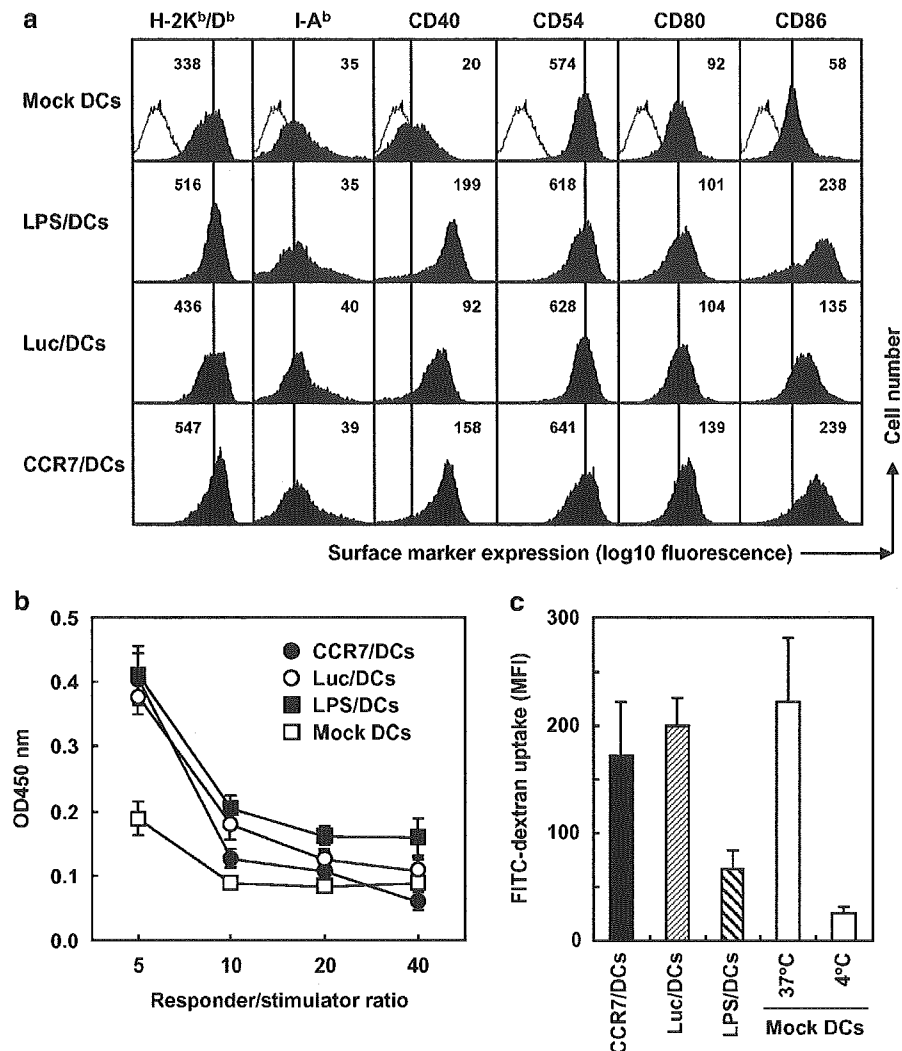
Figure 3 Immunological characteristics of CCR7/DCs. C57BL/6 DCs were transduced with AdRGD-CCR7 or AdRGD-Luc at 50 MOI, and then were cultured for 24 h. (a) These transduced cells, LPS-stimulated DCs, and mock DCs were stained by indirect immunofluorescence using monoclonal antibodies of the indicated specificities (solid histogram). Dotted histograms represent cells stained by phycoerythrin-conjugated streptavidin alone. Values indicated in the upper part of each panel represent MFI of flow cytometric analysis. The data are representative of three independent experiments. (b) Naive BALB/c T lymphocytes were co-cultured with CCR7/DCs, Luc/DCs, LPS/DCs, or mock DCs at the indicated responder/stimulator ratio for 3 days. Cell cultures were pulsed with BrdU during the last 18 h, and then T-cell proliferation was assessed by BrdU-ELISA. Results are expressed as mean±s.e. of three independent cultures using T cells prepared from three individual mice. (c) CCR7/DCs, Luc/DCs, LPS/DCs, and mock DCs were incubated with PBS containing 1 mg/ml FITC-dextran at 4 or 37°C. After 1 h, cells were washed five times with ice-cold PBS and uptake of FITC-dextran was assessed by flow cytometry. MFI of the flow cytometric analysis is presented in the bar chart. Data are presented as the mean±s.d. of four independent cultures.

with the mock DC-treated group. This phenomenon probably reflected the maturation status of Luc/DCs as shown in Figure 3a and b. Importantly, CCR7/DCs could migrate approximately 5.5- and 15-fold more efficiently into the regional LN than Luc/DCs and mock DCs, respectively, clearly demonstrating that CCR7 gene transduction using AdRGD was useful technology to accelerate the accumulation of DC vaccine in regional LN.

Vaccine efficacy of DCs co-transduced with antigen and CCR7

In order to evaluate the potency of CCR7/DCs as vaccine carriers, we prepared the DC vaccine co-transduced with CCR7 gene and ovalbumin (OVA), model antigen, gene using AdRGD. As shown in Figure 5, DCs combined

with AdRGD-OVA and AdRGD-CCR7 could present OVA peptides via MHC class I molecules at levels equal to DCs transduced with AdRGD-OVA alone. On the other hand, the OVA-presentation level in DCs co-transduced with AdRGD-OVA and AdRGD-Luc decreased by half. These data revealed that CCR7 gene transduction did not affect the MHC class I-presentation pathway for antigens endogenously and simultaneously expressed in DCs, and suggested that the proteins accumulating in the cytoplasm and the membrane-localized receptors, such as luciferase and CCR7, respectively, might induce different methods for processing co-expressed endogenous antigens in DCs.

We compared the antitumor effects of DCs co-transduced with gp100, a melanoma-associated antigen, and CCR7 (gp100+CCR7/DCs) and DCs transduced with AdRGD-gp100 alone (gp100/DCs) in the murine
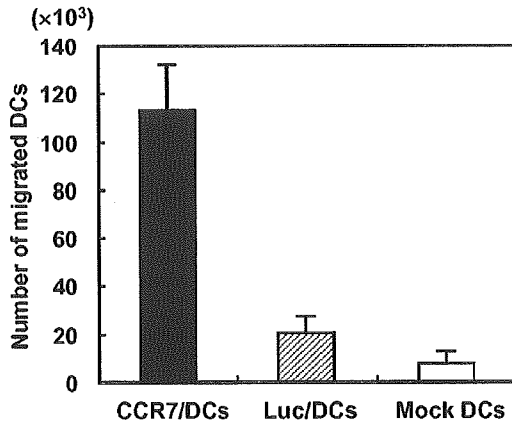
Figure 4 Migration of CCR7/DCs from administration site to draining LN. EGFP-Tg DCs were transduced with AdRGD-CCR7 or AdRGD-Luc at 50 MOI, and then were cultured for 24 h. These transduced cells and mock DCs were intradermally injected into the left flank of C57BL/6 mice at 2×10^6 cells/50 μl. After 2 days, the draining inguinal LNs were collected from these mice, and a single-cell suspension was prepared and stained by indirect immunofluorescence using anti-CD11c monoclonal antibody. The abundance of EGFP$^+$CD11c$^+$ DCs was assessed by flow cytometric analysis acquiring 500 000 events. The number of DCs that had migrated into draining LNs was calculated by multiplying the EGFP$^+$CD11c$^+$ DC frequency by the total number of isolated LN cells. Data are presented as mean±s.e. of results from four mice.
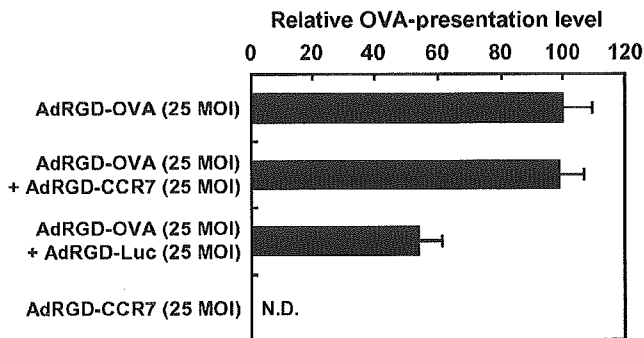

Figure 5 Antigen presentation on MHC class I molecules by CCR7/DCs. DCs were transduced with the indicated combination of AdRGD-OVA, AdRGD-CCR7, and AdRGD-Luc. These cells were co-cultured with CD8-OVA 1.3 cells for 20 h. IL-2 levels released from stimulated CD8-OVA 1.3 cells into culture supernatants were determined by ELISA, and relative OVA-presentation level via MHC class I molecules in each transduced DC was expressed as a percentage of the group using DCs transduced with AdRGD-OVA alone. Data represent the mean±s.d. of three independent cultures. ND: IL-2 secreted from CD8-OVA 1.3 cells was not detectable.

B16BL6 melanoma model. Obvious growth suppression of B16BL6 tumor challenge was achieved in mice vaccinated with gp100/DCs, as shown in our previous report,[14] whereas immunization with mock DCs or CCR7/DCs was not effective (Figure 6). This vaccine efficacy of gp100/DCs depended on the administered DC dosage. Notably, equal antitumor effects were observed in groups vaccinated with 2×10^5 gp100+CCR7/DCs and with 5×10^5 gp100/DCs, and vaccination with 5×10^5 gp100+CCR7/DCs caused extensive inhibition of B16BL6 tumor growth. Thus, we assessed B16BL6-specific CTL activity in mice vaccinated with gp100+CCR7/DCs or gp100/DCs by europium

X   PBS
△   Mock DCs (5×10^5 cells/mouse)
◇   CCR7/DCs (5×10^5 cells/mouse)
○   gp100/DCs (5×10^5 cells/mouse)
□   gp100/DCs (2×10^5 cells/mouse)
●   gp100+CCR7/DCs (5×10^5 cells/mouse)
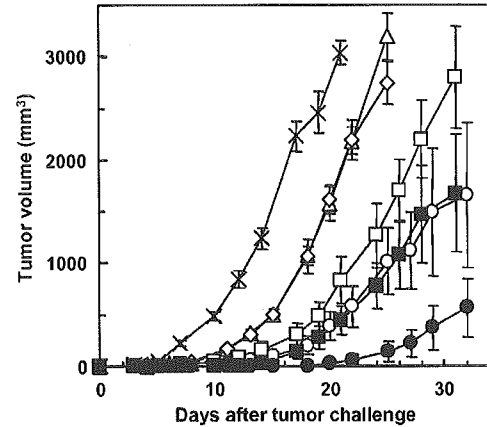▣   gp100+CCR7/DCs (2×10^5 cells/mouse)

Figure 6 Vaccine efficacy of DCs co-transduced with CCR7 and gp100 gene against B16BL6 melanoma challenge. CCR7/DCs, gp100/DCs, and gp100+CCR7/DCs were prepared using corresponding vectors at 25 MOI, and then cultured for 24 h. C57BL/6 mice were immunized by intradermal injection of transduced DCs into the left flank at the indicated cell dosage, and then 4×10^5 B16BL6 melanoma cells were inoculated into the right flank of the mice at 1 week post-vaccination. The tumor sizes were assessed using microcalipers three times per week. Each point represents the mean±s.e. of 5–10 mice.

(Eu)-release assay (Figure 7a). The effector cells prepared from mice vaccinated with gp100/DCs could strongly injure B16BL6 cells, as we reported previously.[14] In addition, the effector cells in all groups did not induce lysis of YAC-1 cells, which are highly susceptible to NK activities, and H-2 haplotype-matched irrelevant EL4 thymoma cells (data not shown). B16BL6-specific cytotoxic activity increased in splenocytes from mice vaccinated with gp100+CCR7/DCs, depending on administered DC-dosage, and cytotoxicity exceeded that observed in the group treated with gp100/DCs at same dosage (5×10^5 cells/mouse). Furthermore, re-stimulated splenocytes from mice vaccinated with gp100+CCR7/DCs at 2 or 5×10^5 cells/mouse exhibited higher frequency of interferon-γ (IFN-γ)-producing cells in ELISPOT assay in comparison with those from 5×10^5 gp100/DCs-immunized mice (Figure 7b). Taken together, these data indicated that the induction of a TAA-specific immune response can be potentiated by the improved migration of TAA-loaded DC vaccine from the administration site to lymphoid tissue.

Discussion

The development of a vaccine for cancer treatment aims for sufficient induction of the tumor-specific immune response, in which antitumor CTLs play a central role, to a level capable of tumor rejection and regression. The
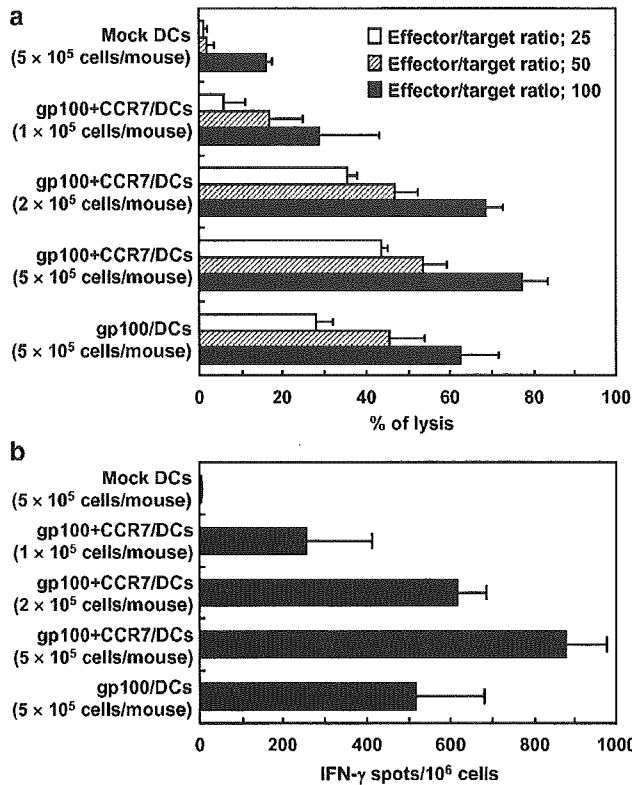
a

b

Figure 7 CTL activity and the frequency of IFN-γ-producing cells in splenocytes from mice immunized with DCs cotransduced with CCR7 and gp100 gene by AdRGD. gp100/DCs and gp100+CCR7/DCs were prepared using corresponding vectors at 25 MOI, and then cultured for 24 h. These transduced cells and mock DCs were vaccinated once intradermally into C57BL/6 mice at the indicated cell dosage. At 1 week after immunization, nonadherent splenocytes were prepared from these mice, and then were re-stimulated in vitro for 5 days with IFN-γ-stimulated and MMC-inactivated B16BL6 cells. (a) A cytolytic assay using the re-stimulated splenocytes (effector cells) was performed against IFN-γ-stimulated B16BL6 cells (target cells). The data represent the mean±s.e. of four independent cultures from four individual mice. (b) IFN-γ-producing cells in re-stimulated splenocytes were evaluated by mouse IFN-γ ELISPOT assay. The data represent the mean±s.d. of results from four mice.

efficient priming and subsequent activation of antitumor CTLs requires the processing and presentation of TAAs as peptide fragments in the context of appropriate MHC class I molecules by APCs.[15] DCs are the most potent APCs and are uniquely capable of presenting novel antigens to naive T cells to initiate and modulate immune responses.[5–7] Owing to these properties, TAA-loaded DCs are considered promising vaccine carriers in immune intervention strategies against cancer. However, very few DCs in currently available DC-based immunotherapies are capable of migrating from an administration site to regional lymphoid tissue,[16–18] where they present MHC class I- and II-restricted peptides to naive T cells, because optimal DC conditioning for enhancing migratory ability is not yet established. Therefore, increasing the migratory ability of a DC vaccine toward lymphoid tissues would remarkably improve the efficacy of DC-based immunotherapy because priming/activation of immune effector cells would be significantly promoted. In the present study, we focused on the chemokine receptor, CCR7, which manages facilitated DC migration to lymphoid tissues, and attempted to

create a DC vaccine that sufficiently expressed CCR7 on the surface by gene transduction.

A vector system that can effectively deliver a foreign gene to DCs is essential for preparing a genetically modified-DC vaccine. We have demonstrated that AdRGD can enhance gene transduction efficiency against murine and human DCs as compared with conventional Ad because of the expression of the RGD sequence, the αv-integrin-targeting peptide, at the HI loop in the fiber knob.[11–14] Therefore, we constructed AdRGD-CCR7, which carried the expression cassette containing mouse CCR7 cDNA under the control of the cytomegalovirus promoter, and confirmed the vector's performance. RT-PCR analysis indicated that transfection using AdRGD-CCR7 allowed murine bone marrow-derived DCs to express abundant CCR7 mRNA, and CCR7 mRNA expression in CCR7/DCs was the highest at 24 h after gene transduction. Furthermore, CCR7/DCs cultured for 24 h exhibited sufficient CCR7 protein expression on the cell surface in flow cytometric analysis and demonstrated strong migratory ability toward CCL21, a CCR7 ligand secreted constitutively from lymphoid tissues, depending on both CCL21 concentration in a 4 h chemotaxis assay and AdRGD-CCR7 dose in transfection. That is, efficient CCR7-gene transduction into DCs by AdRGD reinforced surface expression of CCR7, which sensed a CCL21 concentration gradient and transmitted intracellular signals associated with migration in their original biologically active form. Although DCs generally enhance the expression of CCR7 and acquire migratory ability to lymphoid tissues by various maturation stimuli, an increase in CCR7 mRNA levels and enhancement of migratory activity toward CCL21 were not observed in LPS/DCs, contrary to our expectation. Granucci et al[19] reported that DCs stimulated with LPS significantly decreased their intrinsic migratory ability and increased the antigen uptake function at 1–2 h post-stimulation. This phenomenon probably represents the in vivo stage during which DCs remain at an inflammation site caused by the components of invading bacteria, such as LPS, and capture antigens by full endocytosis. In addition, Granucci et al[19] demonstrated that, at around 4 h after LPS activation, DCs recovered their migratory ability and started to progressively lose antigen uptake function until they reached the mature stage in which LPS/DCs showed poor antigen uptake and migratory activity. Therefore, because in the present study we tested the responses 24 h after LPS stimulation, low CCR7 mRNA levels and poor migratory response to CCL21 by LPS/DCs may have been observed because tests were run after the optimal time point, suggesting that the control of DC-migratory activity by LPS stimulation is difficult.

DCs are strong initiators of defense mechanisms that combat infectious diseases and cancer, but, in their role as APCs, DCs are also involved in immune suppression and immune tolerance.[20–23] In their induction of a positive immune response, immature DCs capture invading antigens at peripheral locations and are then activated by inflammatory stimuli, such as interleukin (IL)-1β, tumor necrosis factor-α, and bacterial components, to migrate to T-cell-rich areas in regional LN. In these processes, DCs enhance the expression of MHC/costimulatory molecules, which is essential for T-cell surface sensitization for effective induction of T-cell-

dependent primary immune responses. On the other hand, in negative immune regulation, immature DCs take up resident biological materials or apoptotic bodies and present processing peptides without acquiring activated phenotypes during migration to regional LN.[24,25] Therefore, a full analysis and understanding of immunological characteristics of DC vaccine is imperative for the development of DC-based immunotherapy because the polarity of the immune response is greatly influenced by the activated state of DCs during T-cell sensitization. CCR7/DCs created in the present study maintained inherent endocytotic activity, suggesting that CCR7/DCs administered into tumor tissue can capture necrotic or apoptotic tumor cell fragments and may induce TAA-specific immune responses. Yanagawa *et al*[26] reported that internalization of FITC-dextran in murine mature DCs increased in the presence of CCR7 ligand, CCL19 or CCL21. These results support the notion that CCL21, secreted from lymphatic vessels located near a tumor, may encourage uptake of tumor cell fragments by CCR7/DCs injected into the tumor tissue. Although high endocytotic activity is a characteristic feature of immature DCs, flow cytometric analysis indicated that CCR7/DCs enhanced expression of MHC/costimulatory molecules and allo-MLR suggested the reinforcement of T-cell proliferation-stimulating ability. These results agreed with our previous report demonstrating that transduction using AdRGD could enhance the maturation status of DCs,[13] strongly suggesting that CCR7 gene transduction using AdRGD did not inhibit the original APC characteristics of DCs and that CCR7/DCs can function as a useful vaccine possessing sufficient T-cell activation ability *in vivo*.

Although a technique to label DCs with radioisotopes or fluorescent substances is frequently used for evaluating *in vivo* kinetics of administered DC vaccines,[27–32] release via exosomes or leakage of the labeling material from DCs complicates the analysis. Eggert *et al*[33] reported that application of EGFP-Tg mouse-derived DCs avoided this problem and enabled simple evaluation and analysis of the kinetics of administered DCs without the need for labeling. Thus, we investigated the migratory ability of CCR7/DCs by flow cytometric analysis of regional LN cells prepared from mice intradermally injected with transduced EGFP-Tg mouse-derived DCs. At 48 h post-injection, regional LNs that served as administration sites for CCR7/DCs were obviously larger than contralateral LNs under macroscopic observation, and the frequency of EGFP⁺CD11c⁺ DCs in regional LN cells was 1.93±0.54, 0.57±0.19, and 0.12±0.04% (mean±s.e.) for CCR7/DCs-, Luc/DCs-, and mock DCs-injected mice, respectively. In addition, we could prepare more cells from regional LN in CCR7/DCs-injected mice than from the Luc/DC or mock DC groups, suggesting that not only administered DCs but also other immune cells, such as T cells, might accumulate in regional LN in mice injected with CCR7/DCs.

Previously, we demonstrated that immunization with DCs efficiently transduced with gp100 gene by AdRGD could significantly inhibit the growth and lung metastasis of murine B16BL6 melanoma *in vivo*.[14] In order to actually evaluate the predominancy of CCR7-transduced DCs as a vaccine carrier *in vivo*, we investigated anti-B16BL6 melanoma effects in mice vaccinated with DCs genetically engineered to simultaneously express gp100

and CCR7. Although antigen presentation via MHC class I molecules in the experiment using AdRGD-OVA was the same for DCs transduced with OVA gene alone and co-transduced with OVA and CCR7 gene, immunization with gp100+CCR7/DCs could more effectively suppress growth of B16BL6 tumors than vaccination with gp100/DCs. Furthermore, DC vaccine co-transduced with the TAA gene and the CCR7 gene effectively induced TAA-specific and IFN-γ-producing CTLs using a lower dosage than conventional DC vaccine transduced with TAA gene alone. These data suggest that augmentation of lymphoid tissue directivity of DCs by efficient CCR7-gene transduction can reduce the DC vaccine dosage that is needed to elicit efficacious therapeutic effects in DC-based immunotherapy. In other words, this method may considerably reduce the cost, time, and effort for DC vaccine preparation and relieve the patient from the burden of frequent blood drawing for DC isolation.

In conclusion, our data strongly suggested that *in vivo* kinetic control of DC vaccine, namely the establishment of an active DC delivery system to lymphoid tissues, was very useful for improving the efficacy of DC-based immunotherapy. We expect that superior lymphoid tissue accumulation of DCs transduced with the CCR7 gene is advantageous for a vaccine carrier because of efficient activation of immune effector cells in regional LNs and a rapid supply of activated effector cells to the whole body. Recently, optimized DC conditioning, which includes stimulation of antigen-presenting DCs with various cytokines or ligand molecules, has been investigated for the development of more effective DC-based immunotherapy. Several reports demonstrated that DC stimulation by prostaglandin E₂[34–36] or the pre-induction of inflammatory response at the DC-administration site[37] was effective in promoting migration of administered DCs to lymphoid tissues. Further research and development of 'lymphoid tissue-directivity DC' vaccine based on these data and our results may greatly improve efficacy and lead to clinical application of DC-based immunotherapy.

Materials and methods

Cell lines and mice

A murine B16BL6 melanoma cell line (H-2ᵇ) was cultured in minimum essential medium supplemented with 7.5% fetal bovine serum (FBS) and antibiotics. The helper cell line, 293 cells, was grown in Dulbecco's modified Eagle medium supplemented with 10% FBS and antibiotics. CD8-OVA 1.3 cells,[38] specific T–T hybridoma against OVA⁺ H-2Kᵇ (kindly provided by Dr CV Harding; Department of Pathology, Case Western Reserve University, Cleveland, OH, USA), were maintained in Dulbecco's modified Eagle medium supplemented with 10% FBS, 50 μM 2-mercaptoethanol, and antibiotics. Female C57BL/6 mice (H-2ᵇ) and female BALB/c mice (H-2ᵈ), aged 7–8 weeks, were purchased from SLC Inc. (Hamamatsu, Japan). EGFP-Tg mice, C57BL/6 TgN(act-EGFP)OsbC14-Y01-FM131,[39] were kindly provided by Dr M Okabe (Genome Information Research Center, Osaka University, Suita, Japan). All mice were held under specific pathogen-free conditions and the experimental procedures were in accordance with the Osaka University guidelines for the welfare of animals in experimental neoplasia.

Vectors

Replication-deficient AdRGD was based on the adenovirus serotype 5 backbone with deletions of E1 and E3 regions. The RGD sequence for αv-integrin targeting was inserted into the HI loop of the fiber knob using a two-step method as described previously.[40] The expression cassette containing mouse CCR7 cDNA derived from pBluescript SK(+)/mCCR7 under the control of the cytomegalovirus promoter was inserted into the E1-deletion site to construct AdRGD-CCR7, using an improved *in vitro* ligation method as described previously.[40–42] Luciferase-expressing AdRGD (AdRGD-Luc), OVA-expressing AdRGD (AdRGD-OVA), and gp100-expressing AdRGD (AdRGD-gp100) were constructed previously.[12–14] All recombinant AdRGDs were propagated in 293 cells, purified by two rounds of cesium chloride gradient ultracentrifugation, dialyzed, and stored at −80°C. Titers of infective AdRGD particles were evaluated by the end-point dilution method using 293 cells.

Mouse bone marrow-derived DCs

DCs were prepared according to the method of Lutz *et al*,[43] with slight modification. Briefly, bone marrow cells flushed from the femurs and tibias of C57BL/6 or EGFP-Tg mice were seeded at 5×10^6 cells per sterile 100-mm bacterial grade culture dish in 10 ml of RPMI 1640 containing 10% FBS, 40 ng/ml recombinant murine granulocyte/macrophage colony-stimulating factor (GM-CSF; kindly provided by KIRIN Brewery Co., Ltd, Tokyo, Japan), 50 μM 2-mercaptoethanol, and antibiotics. On day 3, another 10 ml of culture medium was added to the dish for medium replenishment. On day 6, 10 ml of the culture supernatant was collected and centrifuged at 1500 rpm for 5 min at room temperature, and the pellet was resuspended in 10 ml of fresh culture medium, and then returned to the original dish to conserve unattached cells. Eight-day-old DCs (nonadherent cells) were harvested and used as intact immature DCs in subsequent experiments. DCs cultured for another 24 h with media containing 1 μg/ml LPS (Nacalai Tesque, Inc., Kyoto, Japan) were used as phenotypically mature DCs.

Viral transduction into DCs

DCs were suspended at a concentration of 5×10^6 cells/ml in FBS-free RPMI 1640 and placed in a 15-ml conical tube. Each AdRGD was added at various MOI, the suspension was mixed well, and the tube was incubated at 37°C for 2 h with occasional gentle agitation. The cells were washed three times with phosphate-buffered saline (PBS) and resuspended in a suitable solution.

Semiquantitative RT-PCR analysis

CCR7/DCs, Luc/DCs, and mock DCs were cultured on 100-mm bacterial grade culture dishes in GM-CSF-free culture medium. Mouse CCR7 gene expression was assessed by semiquantitative RT-PCR analysis as follows. Total RNA was isolated from these cells and LPS/DCs using Sepasol-RNA I Super (Nacalai Tesque, Inc.) according to the manufacturer's instructions, and then RT proceeded for 60 min at 42°C in a 50 μl reaction mixture containing 5 μg total RNA treated with DNase I, 10 μl 5 × RT buffer, 5 mM MgCl₂, 1 mM dNTP mix, 1 μM random primer (9-mer), 1 μM oligo(dT)₂₀, and 100 U

ReverTra Ace (TOYOBO Co., Ltd, Osaka, Japan). PCR amplification of the CCR7 and β-actin transcripts was performed in 50 μl of a reaction mixture containing 1 μl of RT material, 5 μl 10 × PCR buffer, 1.25 U *Taq* DNA polymerase (TOYOBO Co., Ltd), 1.5 mM MgCl₂, 0.2 mM dNTP, and 0.4 μM primers. The sequences of the specific primers were as follows; mouse CCR7: forward, 5′-aca gcg gcc tcc aga aga aca gcg g-3′; reverse, 5′-tga cgt cat agg caa tgt tga gct g-3′; mouse β-actin: forward, 5′-tgt gat ggt ggg aat ggg tca g-3′; reverse, 5′-ttt gat gtc acg cac gat ttc c-3′. After denaturation for 2 min at 95°C, 20 cycles of denaturation for 30 s at 95°C, annealing for 30 s at 60°C, and extension for 30 s at 72°C were repeated and followed by completion for 4 min at 72°C. The PCR product was electrophoresed through a 3% agarose gel, stained with ethidium bromide, and visualized under UV radiation. The expected PCR product sizes were 345 bp (CCR7) and 514 bp (β-actin). Quantification of PCR products was performed by densitometry analysis, and the relative CCR7 mRNA expression level was calculated as the ratio of the densitometric units of CCR7 PCR-products to the densitometric units of β-actin PCR products.

Flow cytometric analysis for mouse CCR7

CCR7/DCs and Luc/DCs were prepared by using corresponding vectors at 50 MOI. These transduced DCs, LPS/DCs, and mock DCs were cultured on 100-mm bacterial grade culture dishes in GM-CSF-free culture medium for 24 h. The cells (1×10^6) were fixed by incubation for 10 min in 2% paraformaldehyde, and then incubated with 100 μl staining buffer (PBS containing 0.1% bovine serum albumin and 0.01% NaN₃) containing the anti-FcγRII/III monoclonal antibody (2.4G2; rat IgG₂ᵦ,κ; BD Biosciences, San Jose, CA, USA) to block nonspecific binding of the subsequently used antibody reagents. After 1 h, the cells were incubated overnight with anti-mouse CCR7 polyclonal antibody (goat Ig; ImmunoDetect Inc., Fayetteville, NY, USA) at a 1:10 dilution. Successively, cells were incubated for 2 h with FITC-conjugated rabbit anti-goat Ig (DakoCytomation, Kyoto, Japan) at a 1:100 dilution. Finally, 30 000 events of the stained cells were analyzed for mouse CCR7 protein expression by a FACSCalibur flow cytometer using CellQuest software (Becton Dickinson, Tokyo, Japan). Between all incubation steps, cells were washed three times with staining buffer.

In vitro chemotaxis assay

CCR7/DCs, Luc/DCs, and mock DCs were cultured for 24 or 48 h in GM-CSF-free medium. Chemotactic activity of these DCs and LPS/DCs for CCL21 was measured by an *in vitro* chemotaxis assay across a polycarbonate membrane with 5-μm pores (Chemotaxicell-24; Kurabo Industries Ltd, Osaka, Japan). Recombinant murine CCL21 (PeproTech EC Ltd, London, England) dissolved in an assay medium (RPMI 1640 containing 0.5% bovine serum albumin and 20 mM HEPES) was added to a 24-well culture plate. DCs were suspended with the assay medium and were placed in a Chemotaxicell-24 installed on each well at 10⁶ cells. Cell migration was allowed for 4 h at 37°C in a 5% CO₂ atmosphere. Cells that migrated into the lower compartment were counted using a NucleoCounter™ (ChemoMetec, Allerød, Denmark), and the chemotactic activity was expressed in terms of

the percentage of the input cells calculated by the following formula: (% of input cells) = (the number of migrated cells)/(the number of cells placed in Chemotaxicell-24; 10^6 cells) × 100.

Analysis of surface marker expression

All immunoreagents used in this experiment were purchased from BD Biosciences. CCR7/DCs and Luc/DCs were prepared by using corresponding vectors at 50 MOI. At 24 h after transduction, immunophenotype of transduced DCs, LPS/DCs, and mock DCs was confirmed by flow cytometric analysis. Briefly, 10^6 cells in 100 µl staining buffer were incubated for 30 min on ice with the 2.4G2 monoclonal antibody to block nonspecific binding of the subsequently used immunoreagents. The cells were resuspended in 100 µl staining buffer and incubated for 30 min on ice using the manufacturer's recommended amounts of biotinylated monoclonal antibodies: 28-8-6 (anti-H-2K^b/D^b), AF6-120.1 (anti-I-A^b), 3/23 (anti-CD40), 3E2 (anti-CD54), 16-10A1 (anti-CD80), and GL1 (anti-CD86). The cells were then resuspended in 100 µl staining buffer containing phycoerythrin-conjugated streptavidin at a 1:200 dilution, and nonspecific binding was measured using phycoerythrin-conjugated streptavidin alone. After incubation for 30 min on ice, 30 000 events of the stained cells were analyzed for surface phenotype by flow cytometry. Between all incubation steps, cells were washed three times with staining buffer.

Allogenic MLR

C57BL/6 DCs were transduced with AdRGD-CCR7 or AdRGD-Luc at 50 MOI, and then cultured for 24 h. Allogenic naive T cells were purified from BALB/c splenocytes as nylon wool nonadherent cells, and were used as responder cells at $1 × 10^5$ cells/well in 96-well plates. CCR7/DCs, Luc/DCs, LPS/DCs, or mock DCs (stimulator cells) were inactivated by 50 µg/ml mitomycin C (MMC) for 30 min and added to responder cells in varying cell numbers. Cells were co-cultured in 100 µl RPMI 1640 supplemented with 10% FBS, 50 µM 2-mercaptoethanol, and antibiotics at 37°C and 5% CO_2 for 3 days. Control wells contained either stimulator cells alone or responder cells alone. Cell cultures were pulsed with 5-bromo-2'-deoxyuridine (BrdU) during the last 18 h, and then proliferation of responder cells was evaluated by Cell Proliferation ELISA, BrdU (Roche Diagnostics Co., Indianapolis, IN, USA).

Antigen uptake assay

CCR7/DCs and Luc/DCs were prepared by using corresponding vectors at 50 MOI. These cells, LPS/DCs, and mock DCs were cultured for 24 h, and then resuspended at $5 × 10^6$ cells/ml in ice-cold PBS containing 1 mg/ml FITC-dextran (MW: 77 000; Sigma Chemical Co., St Louis, MO, USA). The cells were incubated at 37 or 4°C to determine background uptake. After 1 h, the cells were washed extensively with ice-cold PBS and analyzed by flow cytometry.

In vivo migration assay

EGFP-Tg mouse-derived DCs were transduced with AdRGD-CCR7 or AdRGD-Luc at 50 MOI, and then cultured for 24 h. These transduced cells and mock DCs were intradermally injected into the left flank of wild-type C57BL/6 mice at $2 × 10^6$ cells/50 µl. After 2 days, the draining inguinal LNs were collected from these mice, and then a single-cell suspension was prepared. The isolated LN cells were blocked by 2.4G2 monoclonal antibody and stained by indirect immunofluorescence with biotinylated anti-CD11c monoclonal antibody (HL3; BD Biosciences) and PerCP-conjugated streptavidin. The stained cells were analyzed by flow cytometry acquiring 500 000 events, and the number of migrated DCs into draining LNs was calculated by multiplying the EGFP$^+$CD11c$^+$ cell frequency by the total number of isolated LN cells.

Antigen-presentation assay

C57BL/6 DCs were transduced with various combinations of AdRGD-OVA, AdRGD-CCR7, and AdRGD-Luc each at 25 MOI, and then seeded on a 96-well flat-bottom culture plate at a density of $1 × 10^5$ cells/well. These cells were co-cultured with $1 × 10^5$ cells/well CD8-OVA 1.3 cells at 37°C for 20 h. The response of stimulated CD8-OVA 1.3 cells was assessed by determining the amount of IL-2 released into an aliquot of culture medium (100 µl) using a murine IL-2 ELISA KIT (Biosource International, Camarillo, CA, USA). Relative OVA-presentation level via MHC class I molecules in each transduced DC was calculated by the following formula: (relative OVA-presentation level) = (IL-2 level in tested group)/(IL-2 level in group using DCs transduced with AdRGD-OVA alone) × 100.

Tumor protection assay

DCs were transduced with AdRGD-CCR7 alone, AdRGD-gp100 alone, or a combination of AdRGD-CCR7 and AdRGD-gp100, each at 25 MOI, and then cultured for 24 h. These transduced DCs and mock DCs were intradermally injected into the left flank of C57BL/6 mice at 2 or $5 × 10^5$ cells/50 µl. At 1 week after the vaccination, $4 × 10^5$ B16BL6 melanoma cells were intradermally inoculated into the right flank of the mice. The major and minor axes of the tumor were measured using microcalipers, and the tumor volume was calculated by the following formula: (tumor volume; mm^3) = (major axis; mm) × (minor axis; mm)^2 × 0.5236. The mice were euthanized when one of the two measurements was greater than 20 mm.

Eu-release assay and ELISPOT assay for B16BL6-specific CTLs

DCs were transduced with AdRGD-gp100 alone or a combination of AdRGD-CCR7 and AdRGD-gp100 at 25 MOI, and then cultured for 24 h. These transduced DCs and mock DCs were administered once intradermally into the left flank of C57BL/6 mice at 1, 2, or $5 × 10^5$ cells/50 µl. At 1 week after immunization, nonadherent splenocytes were prepared from these mice and re-stimulated in vitro using B16BL6 cells, which were cultured in media containing 100 U/ml recombinant murine IFN-γ (PeproTech EC Ltd) for 24 h and inactivated with 50 µg/ml MMC at 37°C for 30 min, at an effector/stimulator ratio of 10 in RPMI 1640 supplemented with 10% FBS, 50 µM 2-mercaptoethanol, and antibiotics. After 5 days, the splenocytes were collected and used as CTL effector cells. Target cells, IFN-γ-stimulated B16BL6 cells, were Eu-labeled and a Eu-release assay

was performed as described previously.[44] Cytolytic activity was determined using the following formula: (% of lysis) = ((experimental Eu release–spontaneous Eu release)/(maximum Eu release–spontaneous Eu release)) × 100. Spontaneous Eu release of the target cells was <10% of maximum Eu release by the detergent. In addition, IFN-γ-producing cells in the re-stimulated splenocytes were detected by using Mouse IFN-γ ELI-SPOT Kit (BD Biosciences) according to the manufacturer's instruction. Splenocytes from unimmunized mice had a frequency of three IFN-γ spots/10^6 cells with or without re-stimulation.

Acknowledgements

References

1 Nestle FO et al. Vaccination of melanoma patients with peptide- or tumor lysate-pulsed dendritic cells. Nat Med 1998; 4: 328–332.

2 Thurner B et al. Vaccination with Mage-3A1 peptide-pulsed mature, monocyte-derived dendritic cells expands specific cytotoxic T cells and induces regression of some metastases in advanced stage IV melanoma. J Exp Med 1999; 190: 1669–1678.

3 Lodge PA et al. Dendritic cell-based immunotherapy of prostate cancer: immune monitoring of a phase II clinical trial. Cancer Res 2000; 60: 829–833.

4 Yu JS et al. Vaccination of malignant glioma patients with peptide-pulsed dendritic cells elicits systemic cytotoxicity and intracranial T-cell infiltration. Cancer Res 2001; 61: 842–847.

5 Banchereau J, Steinman RM. Dendritic cells and the control of immunity. Nature 1998; 392: 245–252.

6 Steinman RM et al. Antigen capture, processing, and presentation by dendritic cells: recent cell biological studies. Hum Immunol 1999; 60: 562–567.

7 Mellman I, Steinman RM. Dendritic cells: specialized and regulated antigen processing machines. Cell 2001; 106: 255–258.

8 Gunn MD et al. Mice lacking expression of secondary lymphoid organ chemokine have defects in lymphocyte homing and dendritic cell localization. J Exp Med 1999; 189: 451–460.

9 Förster R et al. CCR7 coordinates the primary immune response by establishing functional microenvironments in secondary lymphoid organs. Cell 1999; 99: 23–33.

10 Arthur JF et al. A comparison of gene transfer methods in human dendritic cells. Cancer Gene Ther 1997; 4: 17–25.

11 Okada N et al. Efficient gene delivery into dendritic cells by fiber-mutant adenovirus vectors. Biochem Biophys Res Commun 2001; 282: 173–179.

12 Okada N et al. Efficient antigen gene transduction using Arg–Gly–Asp fiber-mutant adenovirus vectors can potentiate antitumor vaccine efficacy and maturation of murine dendritic cells. Cancer Res 2001; 61: 7913–7919.

13 Okada N et al. Gene transduction efficiency and maturation status in mouse bone marrow-derived dendritic cells infected with conventional or RGD fiber-mutant adenovirus vectors. Cancer Gene Ther 2003; 10: 421–431.

14 Okada N et al. Dendritic cells transduced with gp100 gene by RGD fiber-mutant adenovirus vectors are highly efficacious in generating anti-B16BL6 melanoma immunity in mice. Gene Therapy 2003; 10: 1891–1902.

15 Lanzavecchia A. Identifying strategies for immune intervention. Science 1993; 260: 937–944.

16 Lappin MB et al. Analysis of mouse dendritic cell migration in vivo upon subcutaneous and intravenous injection. Immunology 1999; 98: 181–188.

17 Martín-Fontecha A et al. Regulation of dendritic cell migration to the draining lymph node: impact on T lymphocyte traffic and priming. J Exp Med 2003; 198: 615–621.

18 Kleindienst P, Brocker T. Endogenous dendritic cells are required for amplification of T cell responses induced by dendritic cell vaccines in vivo. J Immunol 2003; 170: 2817–2823.

19 Granucci F et al. Early events in dendritic cell maturation induced by LPS. Microbes Infect 1999; 1: 1079–1084.

20 Dhodapkar MV et al. Antigen-specific inhibition of effector T cell function in human after injection of immature dendritic cells. J Exp Med 2001; 193: 233–238.

21 Steinman RM, Nussenzweig MC. Avoiding horror autotoxicus: the importance of dendritic cells in peripheral T cell tolerance. Proc Natl Acad Sci USA 2002; 99: 351–358.

22 Steinbrink K et al. CD4+ and CD8+ anergic T cells induced by interleukin-10-treated human dendritic cells display antigen-specific suppressor activity. Blood 2002; 99: 2468–2476.

23 Mahnke K et al. Immature, but not inactive: the tolerogenic function of immature dendritic cells. Immunol Cell Biol 2002; 80: 477–483.

24 Huang FP et al. A discrete subpopulation of dendritic cells transports apoptotic intestinal epithelial cells to T cell areas of mesenteric lymph nodes. J Exp Med 2000; 191: 435–444.

25 Hemmi H et al. Skin antigens in the steady state are trafficked to regional lymph nodes by transforming growth factor-β1-dependent cells. Int Immunol 2001; 13: 695–704.

26 Yanagawa Y, Onoe K. CCR7 ligands induce rapid endocytosis in mature dendritic cells with concomitant up-regulation of Cdc42 and Rac activities. Blood 2003; 101: 4923–4929.

27 Saeki H, Moore AM, Brown MJ, Hwang ST. Secondary lymphoid-tissue chemokine (SLC) and CC chemokine receptor 7 (CCR7) participate in the emigration pathway of mature dendritic cells from the skin to regional lymph nodes. J Immunol 1999; 162: 2472–2475.

28 Curiel-Lewandrowski C et al. Transfection of immature murine bone marrow-derived dendritic cells with the granulocyte-macropharge colony-stimulating factor gene potently enhances their in vivo antigen-presenting capacity. J Immunol 1999; 163: 174–183.

29 Hirao M et al. CC chemokine receptor-7 on dendritic cell is induced after interaction with apoptotic tumor cells: critical role in migration from the tumor site to draining lymph nodes. Cancer Res 2000; 60: 2209–2217.

30 Wu MT, Hwang ST. CXCR5-transduced bone marrow-derived dendritic cells traffic to B cell zones of lymph nodes and modify antigen-specific immune responses. J Immunol 2002; 168: 5096–5102.

31 Nakamura M et al. Dendritic cells genetically engineered to simultaneously express endogenous tumor antigen and

granulocyte macrophage colony-stimulating factor elicit potent therapeutic antitumor immunity. *Clin Cancer Res* 2002; **8**: 2742–2749.

32 de Vries IJM *et al.* Effective migration of antigen-pulsed dendritic cells to lymph nodes in melanoma patients is determined by their maturation state. *Cancer Res* 2003; **63**: 12–17.

33 Eggert AAO *et al.* Analysis of dendritic cell trafficking using EGFP-transgenic mice. *Immunol Lett* 2003; **89**: 17–24.

34 Scandella E *et al.* Prostaglandin E2 is a key factor for CCR7 surface expression and migration of monocyte-derived dendritic cells. *Blood* 2002; **100**: 1354–1361.

35 Scandella E *et al.* CCL19/CCL21-triggered signal transduction and migration of dendritic cells requires prostaglandin E2. *Blood* 2004; **103**: 1595–1601.

36 Sato M *et al.* Generation of mature dendritic cells fully capable of T helper type 1 polarization using OK-432 combined with prostaglandin E_2. *Cancer Sci* 2003; **94**: 1091–1098.

37 Nair S *et al.* Injection of immature dendritic cells into adjuvant-treated skin obviates the need for *ex vivo* maturation. *J Immunol* 2003; **171**: 6275–6282.

38 Pfeifer JD *et al.* Phagocytic processing of bacterial antigens for class I MHC presentation to T cells. *Nature* 1993; **361**: 359–362.

39 Okabe M *et al.* Green mice as a source of ubiquitous green cells. *FEBS Lett* 1997; **407**: 313–319.

40 Mizuguchi H *et al.* A simplified system for constructing recombinant adenoviral vectors containing heterologous peptides in the HI loop of their fiber knob. *Gene Therapy* 2001; **8**: 730–735.

41 Mizuguchi H, Kay MA. Efficient construction of a recombinant adenovirus vector by an improved *in vitro* ligation method. *Hum Gene Ther* 1998; **9**: 2577–2583.

42 Mizuguchi H, Kay MA. A simple method for constructing E1- and E1/E4-deleted recombinant adenoviral vectors. *Hum Gene Ther* 1999; **10**: 2013–2017.

43 Lutz MB *et al.* An advanced culture method for generating large quantities of highly pure dendritic cells from mouse bone marrow. *J Immunol Methods* 1999; **223**: 77–92.

44 Okada N *et al.* Administration route-dependent vaccine efficiency of murine dendritic cells pulsed with antigens. *Br J Cancer* 2001; **84**: 1564–1570.

Immunological properties and vaccine efficacy of murine dendritic cells simultaneously expressing melanoma-associated antigen and interleukin-12

Naoki Okada,[1] Sayaka Iiyama,[1] Yuka Okada,[2] Hiroyuki Mizuguchi,[3] Takao Hayakawa,[4] Shinsaku Nakagawa,[5] Tadanori Mayumi,[5] Takuya Fujita,[1] and Akira Yamamoto[1]

[1]Department of Biopharmaceutics, Kyoto Pharmaceutical University, 5 Nakauchi-cho, Misasagi, Yamashina-ku, Kyoto 607-8414, Japan; [2]Research Institute for Microbial Diseases, Osaka University, 3-1 Yamadaoka, Suita, Osaka 565-0871, Japan; [3]Division of Cellular and Gene Therapy Products, National Institute of Health Sciences, 1-18-1 Kamiyoga, Setagaya-ku, Tokyo 158-8501, Japan; [4]National Institute of Health Sciences, 1-18-1 Kamiyoga, Setagaya-ku, Tokyo 158-8501, Japan; and [5]Department of Biopharmaceutics, Graduate School of Pharmaceutical Sciences, Osaka University, 1-6 Yamadaoka, Suita, Osaka 565-0871, Japan.

Interleukin (IL)-12 is a key factor for inducing cellular immune responses, which play a central role in the eradication of cancer. In the present study, in order to create a dendritic cell (DC)-based vaccine capable of positively skewing immune response toward a cellular immunity-dominant state, we analyzed immunological characteristics and vaccine efficacy of DCs cotransduced with melanoma-associated antigen (gp100) and IL-12 gene (gp100 + IL12/DCs) by using RGD fiber-mutant adenovirus vector (AdRGD), which enables highly efficient gene transduction into DCs. gp100 + IL12/DCs could simultaneously express cytoplasmic gp100 and secretory IL-12 at levels comparable to DCs transduced with each gene alone. In comparison with DCs transduced with gp100 alone (gp100/DCs), upregulation of major histocompatibility complex class I, CD40, and CD86 molecules on the cell surface and more potent T-cell-stimulating ability for proliferation and interferon-γ secretion were observed as characteristic changes in gp100 + IL12/DCs. In addition, administration of gp100 + IL12/DCs, which were prepared by a relatively low dose of AdRGD-IL12, could induce more potent tumor-specific cellular immunity in the murine B16BL6 melanoma model than vaccination with gp100/DCs. However, antitumor effect and B16BL6-specific cytotoxic T-lymphocyte activity in mice vaccinated with gp100 + IL12/DCs diminished with increasing AdRGD-IL12 dose during gene transduction, and paralleled the decrease in presentation levels via MHC class I molecules for antigen transduced with another AdRGD. Collectively, our results suggested that optimization of combined vector dose was required for development of a more efficacious DC-based vaccine for cancer immunotherapy, which relied on genetic engineering to simultaneously express tumor-associated antigen and IL-12.
Cancer Gene Therapy (2005) 12, 72–83. doi:10.1038/sj.cgt.7700772
Published online 24 September 2004

Dendritic cells (DCs) are potent professional antigen-presenting cells (APCs) that play a pivotal role in directing and amplifying the adaptive immune response to pathogens and infected/mutated cells.[1,2] The ability of DCs to stimulate naive T cells has long been thought to be crucial in initiating an effective immune response, and DCs are uniquely situated at the interface between the innate and adaptive immune systems. Because of these immunological properties, DCs are currently under intense scrutiny as potential adjuvants for vaccines in

many clinical settings. Studies in healthy volunteers and patients with cancer have shown that tumor-associated antigen (TAA)-pulsed DCs can boost both CD8+ and CD4+ T-cell responses in vivo.[3–5]

Although these promising findings encourage the development of DC-based immunotherapy for cancer, the establishment of DC-manipulation capable of supplementing optimal vaccine function is required for the achievement of sufficient efficacy in current therapy. We previously established a highly efficient gene transduction technique into DCs by applying RGD fiber-mutant adenovirus vector (AdRGD),[6,7] and demonstrated that DCs transduced with TAA gene using AdRGD are effective vaccine carriers for induction of tumor-specific immune responses in mice.[8,9] These results suggested that the AdRGD system is very useful for DC-manipulation